Dissertation

IDENTIFICATION OF Z-CRYSTALLIN/NADPH:QUINONE REDUCTASE AS A RENAL GLUTAMINASE MRNA PH-RESPONSIVE ELEMENT BINDING PROTEIN

Submitted by

Aimin Tang

Department of Biochemistry and Molecular Biology

In partial fulfillment of the requirements

For the degree of Doctor of Philosophy

Colorado State University

Fort Collins, Colorado

Fall, 2001

ProQuest Information and Learning Company
300 North Zeeb Road
P.O. Box 1346
Ann Arbor, MI 48106-1346

COLORADO STATE UNIVERSITY

October 29, 2001

WE HEREBY RECOMMEND THAT THE DISSERTATION PREPARED UNDER OUR SUPERVISION BY AIMIN TANG ENTITLED IDENTIFICATION OF Z-CRYSTALLIN/NADPH:QUINONE REDUCTASE AS A RENAL GLUTAMINASE MRNA PH-RESPONSIVE ELEMENT BINDING PROTEIN BE ACCEPTED AS FULFILLING IN PART REQUIREMENTS FOR THE DEGREE OF DOCTOR OF PHILOSOPHY

Committee on Graduate Work

James R Bamburg

Robert W. Woody

Donald L. Myhres

Advisor

Department Head

ABSTRACT

IDENTIFICATION OF Z-CRYSTALLIN/NADPH:QUINONE REDUCTASE AS A RENAL GLUTAMINASE MRNA PH-RESPONSIVE ELEMENT BINDING PROTEIN

During chronic metabolic acidosis, glutamine metabolism increases significantly in rat kidney. This adaptation results in an increase in ammoniagenesis and gluconeogenesis, which facilitate excretion of acid and restoration of blood pH. This response is sustained, in part, by a selective stabilization of glutaminase (GA) mRNA. Previous studies identified an AU-rich element (AURE) located within the 3'-UTR of the GA mRNA. Expression of various chimeric mRNAs in the LLC-PK_1-F^- cells demonstrated that the AURE is both necessary and sufficient to impart a pH-responsive stabilization, and is therefore considered a pH-responsive element (pHRE). Using RNA-EMSA, this pHRE was found to bind to a cytosolic protein with a high affinity and specificity. A biotinylated oligoribonucleotide containing the pHRE was used as an affinity ligand to purify a 36-kDa protein from rat renal cortex that exhibited the same specific binding properties as observed with crude cytosolic extracts. MS/MS micorsequencing identified multiple peptides that were either identical or highly homologous to mouse ζ-crystallin/NADPH:quinone reductase. Antiserum against ζ-crystallin cross-reacts with the purified protein. This serum also blocks the formation of the protein/RNA complex between the pHRE and a crude extract. Bacterially expressed recombinant ζ-crystallin was purified, but it failed to form a complex with pHRE. However, there was indication that this protein, when expressed in LLC-PK_1-F^-, retained

the affinity to pHRE. Thus, the combined data indicate that ζ-crystallin is the rat renal GA mRNA pH-responsive element binding protein (pHRE-BP).

Aimin Tang

Department of Biochemistry

And Molecular Biology

Fort Collins, CO 80523

Fall, 2001

ACKNOWLEDGEMENTS

My foremost acknowledgement goes to my advisor, Dr. Norman Curthoys, for his dedicated support during my graduate career. I had benefited from the many thought-provoking discussions with him throughout the project. What I value most is the opportunity to absorb his love for science, wisdom into specifics and care to everyone around him.

I next thank the members of my committee for their time and energy in helping me improve this document: Dr. James Bamburg, Dr. Robert Woody, Dr. Paul Laybourn, and Dr. Donald Mykles. I also enjoyed learning from them in many other ways as well.

Dr. Omar Laterza laid a solid foundation for this project. He and many other people from the lab gave me tremendous help in experimental skills. I also want to thank Dr. Andrea Terrell from the Laybourn lab for leading me through numerous FPLC purifications, and Laurie Minamide from the Bamburg lab for her help in 2-dimensional electrophoresis.

Thanks to many current and former people from the Curthoys lab for their friendship over the years, including: Omar Laterza, Xiangdong Liu, Lynn Taylor, Tom Holcomb, Quynh Wall, Cliff Hall, Jill Schroeder, Hend Ibrahim, Wenlin Liu and many undergraduate students.

Last but not least, I acknowledge the love and support of my family during the relatively long process of going through this degree program. More over, I thank my wife, Ruiying, for her constant support I needed in completing this dissertation.

TABLE OF CONTENT

FIGURES AND TABLES

ABBREVIATIONS

AURE – AU-rich element

b – base(s)

bp – base pair(s)

βG - β globin

CAT – chloramphenicol acetyltransferase

cDNA – complementary deoxyribonucleic acid

DEPC – diethylpyrocarbonate

DNA – deoxyribonucleic acid

DRB – 5,6-dichloro-1-b-D-ribofuranosyl-benzimidazole

DTT – dithiothreitol

EDTA – ethylenediaminetetraacetic acid

EMSA – electrophoretic mobility shift assay

ERK – extracellular signal-related kinase

FPLC – fast performance liquid chromatography

GA – glutaminase

GAPDH – glyceraldehyde-3-phosphate dehydrogenase

GDH – glutamate dehydrogenase

IRE – iron responsive element

JNK – jun N-terminal kinase

kDa – kilodalton

MAPK – mitogen-activated protein kinase

mRNA – messenger ribonucleic acid

NAD^+ - nicotinamide adenine dinucleotide, oxidized form

NADH – nicotinamide adenine dinucleotide, reduced form

$NADP^+$ - nicotinamide adenine dinucleotide phosphate, oxidized form

NADPH – nicotinamide adenine dinucleotide phosphate, reduced form

PABP – poly(A) binding protein

PBS – phosphate saline solution

PEPCK – phosphoenolpyruvate carboxykinase

pHRE – pH-responsive element

pHRE-BP – pH-responsive element binding protein

REP sequence – repetitive extragenic palindromic sequence.

RNA – ribonucleic acid

RNAsin – RNase inhibitor

SDS – sodium dodecylsulfate

TAE – tris acetate EDTA

TBE – tris borate EDTA

TIAR – T-cell restricted intracellular antigen-related protein

UTR – untranslated region

ζ-crystallin – or NADPH-dependent quinone reductase (EC 1.6.-.-)

1. Introduction

1. INTRODUCTION

1.1. Glutamine and its biological function

Glutamine is one of the two amide-bearing amino acids among the 20 "standard" amino acids. It is used as a substrate in many enzymatic reactions and is synthesized from glutamate and ammonia by glutamine synthetase (Curthoys and Watford, 1995). Because of its high rate of *in vivo* synthesis, it was initially classified as a non-essential amino acid. However, the endogenous storage and synthesis of glutamine may not always meet the demand, especially in patients suffering critical illnesses such as during recovery from major surgery, trauma or sepsis. Its effectiveness in treating patients with such conditions has led to its reclassification as a conditionally essential amino acid (Neu et al., 1996).

Glutamine accounts for 4.3% of the composition of the average proteins. In contrast, it is the most abundant free amino acid in the body, where it constitutes 60% of the total pool (Curthoys and Watford, 1995). Glutamine plays an important role as a precursor for the biosynthesis of various nitrogen-containing compounds, and as a metabolic fuel. Depending on the cell type, the metabolic pathway and function for glutamine can be very different.

Glutamine is utilized in all cells for the syntheses of purines, pyrimidines, glucosamine and other amino acids (Haussinger, 1998; McCauley et al., 1999; Newsholme et al., 1997; Kvamme, 1984; and Colquhoun et al., 1997). However, in many cells, such as the absorptive epithelial cells of the small intestine, cells of the immune system, the fetus, hair follicles and many tumors, the various glutamine-dependent amidotransferase reactions account for less than 5% for the total glutamine extracted. The

majority of the glutamine consumed in these cells is utilized as a respiratory fuel. In the intestinal cells, glutamine is only partially oxidized. Products generated from its catabolism, such as lactate, alanine and aspartate, are utilized by other tissues (Watford, 1994).

In the brain, glutamine can be hydrolyzed by glutaminase to produce neurotransmitter substances (Bradford et al., 1978 and Weiler et al., 1979). This occurs in the terminals of neurons where glutaminase activity is high. The hydrolysis reaction yields glutamate, one of the most abundant neuroexcitatory substances. Decarboxylation of the resulting glutamate yields γ-aminobutyric acid, an important neuroinhibitory substance. These transmitters are released by acidnergic neurons and are taken up by glial cells where glutaminase activity is low and glutamine synthetase activity is high. Thus, glutamine is resynthesized through an intercellular cycle (Kvamme et al., 1991).

In liver, glutamine synthetase is expressed solely in a 1- to 3-cell layer of hepatocytes that surrounds the venous end of the acinus, whereas glutaminase is located predominantly in periportal cells (Gebhardt et al., 1993 and Watford et al., 1990). This compartmentalization is essential for utilizing glutamine to generate glucose and urea and the effective removal of ammonium ions that escape urea synthesis. Liver is also an important organ for glutamine homeostasis. It converts from a net consumer to a net producer of glutamine when other tissues exhibit increased glutamine utilization.

The kidney extracts and metabolizes very little glutamine during normal acid-base balance (Squires et al., 1976). However, metabolic acidosis induces an increased glutamine extraction, which is catabolized primarily in the S1 and S2 segments of the proximal convoluted tubule (Silbernagl, 1980). Glutaminase and glutamine synthetase are

also compartmentalized in the kidney (Burch et al., 1978). Glutamine synthetase is expressed only in the proximal straight tubules (S3 segment), whereas glutaminase activity is highest in distal convoluted and proximal tubules. During acute and chronic acidosis, renal ammoniagenesis and gluconeogenesis are greatly increased. This response generates ammonium and bicarbonate ions that facilitate the excretion of acids and partially restore normal pH balance, respectively.

1.2. Glutaminase

Glutamine is used as a substrate in many enzymatic reactions. However, only one enzyme yields stoichiometric amounds of glutamate and ammonia (shown in the following equation). The enzyme that catalyzes this reaction is recognized as a true glutaminase.

$$\textbf{L-glutamine} + H_2O \rightarrow \textbf{L-glutamate} + NH_4^+$$

There are two major isoenzymes that have the same activity, but differ in sequence, structure, and kinetics (Curthoys and Watford, 1995). This was first noted in 1935, when Krebs indicated that glutaminase activity of liver differed from that of kidney and brain. Later studies revealed that the rat kidney-type enzyme is expressed in kidney, brain, intestine, and fetal liver, while the rat liver-type enzyme is expressed solely in postnatal liver. The distinct genes that encode the two isoforms exhibit > 70% identity within their coding region. From the deduced amino acid sequences the two proteins exhibite > 75% identity between the two (Curthoys and Watford, 1995). Thus, they are the products of different but related genes.

A cDNA for the rat kidney-type glutaminase was isolated by screening cDNA libraries (Shapiro et al., 1991). The full-length cDNA contains 60 bp of 5'-untranslated region, 2022 bp of the coding region, and 2445 bp of the 3'-untranslated region. When expressed, it produces a 74-kDa peptide that is translocated into mitochondria and proteolytically processed to a 72-kDa intermediate. This intermediate is further alternatively processed to produce either a 66- or a 68-kDa mature peptide (Srinivasan et al., 1995). This conclusion is supported by the observation that glutaminase purified from rat brain contains a 3:1 mixture of 66- and 68-kDa peptides, respectively (Shapiro et al., 1991). In addition, antibodies raised against the 66-kDa glutaminase cross-react with both peptides (Shapiro et al., 1987).

1.3. Metabolic acidosis

Under normal condition the kidney extracts and metabolizes very little plasma glutamine. However, this process is rapidly induced by acidosis. Within 1 to 3 h of acute acidosis, plasma glutamine concentration is increased by 2-fold, largely due to glutamine release from the muscle (Hughey et al., 1980 and Schrock et al., 1980). Acidification also activates the α–ketoglutarate dehydrogenase leading to a decrease in intracellular α-ketoglutarate and glutamate (Lowry et al., 1980). The increased availability of the substrate and the decreased concentration of the product increase flux through the glutaminase reaction. Further, the apical Na^+/H^+ antiporter is activated to acidify the urine and facilitate removal of ammonium ions (Horie et al., 1990 and Sastrasinh, 1990).

During chronic acidosis, most of the adaptations are partially compensated. The arterial plasma glutamine concentration is decreased to 65% of the normal level.

However, the kidney extracts and metabolizes about one-third of the plasma glutamine in a pass through this organ (Brosnan et al., 1988 and Squires et al., 1976). This continued catabolism is sustained by the coordinate increases in the mitochondrial glutaminase, the glutamate dehydrogenase, the cytoplasmic phosphoenolpyruvate dehydrogenase, and the Na^+/H^+ and the $Na^+/3HCO_3^-$ transport systems that occur solely within the proximal convoluted tubule (Curthoys et al., 1973; Wright et al., 1990; Burch et al., 1978; and Preisig et al., 1988). The increased renal ammoniagenesis from glutamine generates an expendable cation that facilitates excretion of titratable acids. When α-ketoglutarate is further converted to glucose, HCO_3^- ions are generated and released into the renal venous blood, which partially compensate the acidosis. This process is summarized in Fig. 1.1.

The increase in renal glutaminase activity is most significant within the proximal convoluted tubule. Within 24 h glutaminase activity increases to 2-fold of its normal level. This increase continues gradually if the acidosis persists, but it plateaus after 7 d at a level of 7- to 20-fold greater than normal (Wright et al., 1990). This analysis was confirmed by a microdissection experiment using various segments of the rat nephron. When incubated with glutamine, only the S1 and S2 segments of the proximal tubule dissected from an acidotic animal exhibit an increase in ammonia generation (Good et al., 1984).

The transcription rate of the glutaminase (GA) gene is largely unaffected by changes in acid-base balance, as is indicated in a nuclear run-on assay (Hwang et al., 1991). Rather, the stability of GA mRNA is increased in a time profile that correlates with the increase in GA mRNA levels (Hwang et al., 1991). Both forms of rat GA mRNA, which are produced by use of alternative polyadenylation sites, exhibit a

Fig. 1.1. Responses in a proximal tubule cell during chronic acidosis.

The increased activity in gluconeogenic and ammoniagenic pathways are shown in thicker arrows (From Dr. Laterza's Ph.D. thesis, 1998)

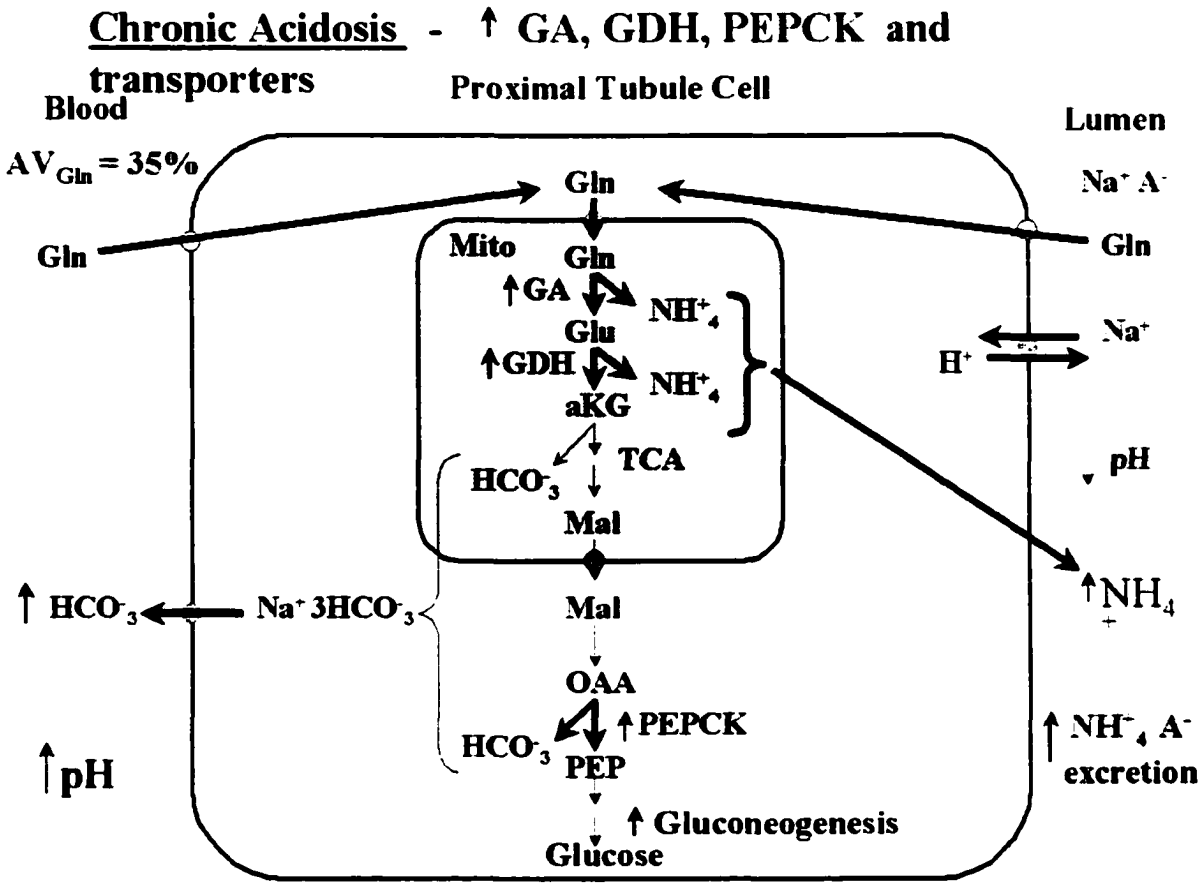

Fig. 1.1

coordinate response to changes in acid-base balance. The stabilization of the GA mRNA was initially demonstrated by stable transfection of various β-globin (βG) constructs into LLC-PK_1-F^- cells, a pH-responsive porcine proximal tubule-like cell line (Hansen et al., 1996). βG mRNA is expressed at a high level with $t_{1/2}$ of >30h. In contrast, βG-GA, which has an additional 955-base sequence (2009-2963) from the 3'-UTR of GA mRNA inserted after the β–globin coding region, is expressed at a low level, and has a much faster turnover rate ($t_{1/2}$=4.6 h). Transferring the cells into acidic medium stabilizes βG-GA mRNA, leading to a half-life of 29 h.

1.4. mRNA stability regulation in eukaryotic cells

1.4.1. mRNA degradation pathway

The measurement of mRNA stability is its half-life ($t_{1/2}$), which is defined as the time required for half of the mRNA to be degraded. In mammalian cells, this value can vary significantly, ranging from 15-30 min for labile mRNAs to longer than 24 h for very stable mRNAs. For a particular mRNA, the stability can be controlled by specific interactions between sequence elements and RNA-binding proteins in response to developmental or environmental stimuli such as nutrients, cytokines, hormones, and environmental stresses such as viral infection, tissue injury, hypoxia, hypocalcemia, and pH (Ross, 1996).

Altered mRNA stability may directly result in the change of the level of the encoded protein. Thus, the whole cell can shift to a new steady state where production and degradation of this protein balance at a new level in response to the changing

environment. The length of this process is, again, dependent on the mRNA itself. Messenger RNAs that encode quick-response proteins must have a short half-life, so that induction in response to a stimulus can be achieved rapidly (Schiavi, 1992 and Paulding, 2000).

Recent research using prokaryotic cells has identified some cis-acting elements that are major contributors in mRNA degradation. These include stable stem-loop structures at either end of the transcript or REP sequences at the 3'-end. Trans-acting elements include two endonucleases (RNase E and RNase III), two exonucleases (PNPase and RNase II), and poly(A) polymerase (Grunberg-Manago, 1999). The rate-limiting step in many cases is an endonucleolytic cleavage by RNase E or, less often, by RNase III, usually occurring near the 5' end. This is generally followed by degradation by the two exonucleases.

In *E. coli*, the key enzyme in controlling mRNA decay is RNase E that with PNPase, is found in a multienzyme complex. These two enzymes work closely to give degradation an apparent 5'-3' polarity. At first, this observation was surprising because PNPase exhibits a 3'-5' polarity. However, RNase E, which requires the free 5' end, catalyzes the first endonucleolytic digestion. The upstream fragment is further digested by PNPases, while the downstream fragment, with a new free 5' end, is processively degraded by RNase E endonuclease (Grunberg-Manago, 1999). *E. coli* uses this divide-and-conquer strategy. As a result, the process appears to have a 5'-to 3' direction.

In many cases, fusing a stable stem-loop structure to the 5' end of a chimeric RNA confers stability (Fournier et al., 2001). However, this is not always true, indicating that the 5' structure is not the only determinant. A 3' stem-loop can act as barrier to

exonucleolytic digestion. Usage of both a 5'- and a 3'-stabilizing element should provide enough protection from cellular degradation machinery in *E. coli* (Grunberg-Manago, 1999).

Eukaryotic mRNAs commonly possess two distinct structures: a 5'-cap and a 3'-poly(A) tract. Their decay usually involves the cooperation of a sequence determinant and a trans-acting protein that interacts with the cis-acting element. Although exceptions exist, for many eukaryotic mRNAs, degradation begins with poly(A) shortening, which is the most likely the rate-limiting step in its turnover (Colgan et al., 1997 and Ono et al., 2000). The next step is usually the cleavage of one or two nucleotides from the 5' end, thereby removing the 5'-cap. The uncapped and deadenylated mRNA is subsequently digested by a 5'-3' exoribonuclease.

In eukaryotic cells, mRNA degradation is often closely related to translation (Jacobson et al., 1996). This is supported by the following data: 1. Inhibitors of translation elongation also retard mRNA decay. 2. Poly(A) tail and PABP are suggested to play a role in translation as well. For example, in electroporated tobacco and microinjected *Xenopus* oocytes, adenylated mRNAs show a substantially higher rate of translation than unadenylated mRNAs. 3. A stable mRNA can be rapidly degraded following the occurrence of an aberrant translation. For example, introduction of a mutation that generates a premature termination causes the mRNA to be quickly degraded in both prokaryotes and eukaryotes. This regenerates the misused nucleotides and conserves energy.

A protein complex that binds to major coding region determinant (mCRD) in c-fos mRNA is proposed to interact with the poly(A) tail (Grosset et al., 2000). According

to this model, formation of such a complex stabilizes the mRNA by protecting the poly(A) tail. However, during translation, this complex may be restructured so that the PABPs dissociate from the poly(A) tail, promoting its degradation. This model explains why translation inhibition always leads to increased mRNA stability.

1.4.2. Regulation of mammalian mRNA degradation

Various conditions can affect mRNA stability. For example, the c-myc mRNA is destabilized during differentiation in C2C12 myoblasts (Yielding et al., 1997). The stability of procollagen mRNA is regulated by hormones such as glucocorticoid and transforming growth factor β (TGFβ) (Raghow et al., 1986, 1987). The cholesterol 7-α-hydroxylase (CYP7A1) mRNA responds to diurnal cycles (Lavery et al., 1993; Lee et al., 1994; and Noshiro et al., 1990). Hypoxia stabilizes lactate dehydrogenase A (LDH-A) mRNA (Short et al., 2000).

Deregulation of mRNA turnover can cause diseases. For example, of the two isoforms of cyclooxygenases, COX1 is constitutively active while COX2 is normally expressed at a very low level. Growth factors, cytokines and tumor promoters can upregulate COX2 expression by inducing the interaction between an AU-rich element in its 3'-UTR and AU-binding proteins that stabilize this mRNA. Stabilization leads to unregulated conversion of free arachidonic acid to prostaglandins which contributes to the development of a carcinoma (Dixon et al., 2000).

1.5. cis- and trans- elements that affect mRNA stability

Work over the last two decades has produced considerable information regarding the process of mRNA degradation. Elements that affect mRNA stability in cis through interaction with certain proteins are found throughout the mRNA. However, more is known about elements in the 3'-UTR than those in the 5'-UTR or in the coding region. Some of the more thoroughly studied cases are presented below.

1.5.1. 3'-UTR elements and their binding proteins

1.5.1.1. poly(A) tract and poly(A)-binding protein (PABP)

A 3'-poly(A) tract in an mRNA is seldom seen at the prokaryotic level but it is a common structure in eukaryotic cells. Normally after transcription, cleavage and polyadenylation specificity factor (CPSF) will bind to the AUUAAA signal and interact with cleavage stimulation factor (CstF) that facilitates binding and stabilizes the ternary complex. The formed complex then recruits a ribonuclease to the cleavage site. CPSF may also activate poly(A) polymerase to synthesize a stretch of poly(A) from ATP (Colgan et al., 1997).

Polyadenylation is not required for translation, as indicated by *in vitro* studies. However, the poly(A) tail and its binding proteins (PABPs) are proposed to be stabilizing factors for mRNA, based on the following observations. 1. The length of poly(A) tail decreases as an mRNA ages. In fact, deadenylation is the first step in the degradation of many mRNAs. Messenger RNAs that lack poly(A) tails, such as histone mRNAs, have short half-lives. 2. PABPs protect the poly(A) tail from destruction. In a cell-free system

that contains mRNA and mRNA-degrading nucleases, depleting PABP results in a rapid mRNA turnover. In contrast, addition of exogenous PABP stabilizes the added mRNA substrates (Jacobson, 1996).

Yeast messenger RNAs also have a poly(A) tail and the corresponding binding protein. However, yeast poly(A) nuclease (PAN) appears to be dependent on PABP for its poly(A) shortening activity. This obvious discrepancy with the above observations is not fully understood.

1.5.1.2. AU-rich elements and AUBPs

A large number of unstable mRNAs have regions that are rich in adenosine and uridine residues (Chen et al., 1995). Many of them, such as the c-fos AU-rich element (AURE), contain two domains. Domain I contains 40-50 nucleotides. Such domains are AU-rich, frequently containing AUUUA pentamers, some of which may overlap. Domain II is located near domain I and has a 20-nucleotide U-rich sequence. In some other cases, domain I is present but domain II is not. There are yet other AUREs, such as those found in c-jun mRNA, that contain AU-rich regions, but lack the AUUUA pattern (Jacobson, 1996).

AUREs are considered RNA instability elements, based on the following findings: 1. They appear in many short-lived mammalian mRNAs, such as proto-oncogenes and cytokines. 2. Appending the AUREs (such as the one from granulocyte-macrophage-colony stimulating factor, or GM-CSF) to a stable mRNA (such as β-globin) will accelerate its decay (Chen et al., 1995).

Most AUREs accelerate deadenylation as the first step in mRNA degradation. However, deadenylation exhibits two different kinetic patterns, distributive and processive, and this difference is not the result of the presence or absence of AUUUA pentanucleotides (Xu et al., 1997). In distributive degradation, which is shown in c-jun and c-fos mRNA degradation, mRNAs start their degradation at the same time and undergo synchronous shortening of the poly(A) tract. However, in processive degradation, represented by GM-CSF, mRNAs are degraded asynchronously, forming a heterogeneous mixture of products with variant lengths. The mechanism behind this difference is not clear yet. However, it suggests the involvement of multiple proteins in mediating the destabilizing effect of AU-rich elements (Chen et al., 1995).

A family of AURE-binding proteins has been described over the last decade. The first one, AUF1, was isolated from erythroleukemic K562 cell line (Brewer, 1991). AUF1 can form a multi-subunit complex with itself or with other factors such as eIF4G, PABP, or hsp70. It was shown to accelerate c-myc mRNA destruction in an *in vitro* study. Interestingly, AUF1 may also participate in the stabilization of some mRNAs, such as the α-globin mRNA that contains a C-rich element and the hypocalcemia-induced parathyroid hormone (PTH) mRNA that contains an AU-rich region (Kiledjian, 1997 and Sela-Brown, 2000).

Another class of AURE-binding proteins closely relates to the *Drosophila* neuron-specific RNA-binding protein ELAV. These include Hel-N1, HuC, HuD and HUD which function to stabilize the mRNAs (Ma et al., 1997). Additional AURE-binding proteins include tristetraproline, a zinc-finger protein with two CCCH zinc finger domains that destabilizes TNF-α, GM-CSF, and IL-3 mRNAs (Ono et al., 2001), and glyceraldehyde-

3-phosphate dehydrogenase (GAPDH), which was first isolated from human spleen, that binds specifically to IFN-γ 3'-UTR (Nagy et al., 1995).

1.5.1.3. Stem-loop structure recognized by iron-regulatory protein (IRP)

Some mRNAs form specific stem-loop structures that binds specific proteins, and function as a stabilizing element. For example, the 3'-UTR of the transferrin receptor (TfR) mRNA contains five iron-responsive elements (IREs). Each IRE consists of a 23 to 27-bp stem plus a six-nucleotide loop. Two cytosolic proteins, iron regulatory proteins 1 and 2 (IRP1 and IRP2), recognize this structure. Under low cellular iron concentration, IRP1 and IRP2 bind to the IREs in TfR mRNA 3'-UTR. This binding protects it from degradation, leading to enhanced iron uptake. At the same time, IRP1 and IRP2 can bind to the IRE in the 5'-UTR of ferritin mRNA, blocking its translation initiation and preventing iron sequestration. When cellular iron level becomes high, the above processes are reversed to lower iron uptake and increase iron sequestration (Rouault et al., 1997).

1.5.1.4. Other stem-loop structures

For insulin-like growth factor II mRNA, a complex stem-loop structure is formed in its 3'-UTR that spans over 2 kb in sequence. This is a very stable structure, with ΔG^{o} of −100 kcal/mol. This structure, directly or indirectly, recruits an endonuclease that generates a very stable 3' cleavage product of 1.8 kb and an unstable 5' coding region that is subjected to rapid degradation.

The stability of histone mRNAs varies with different phases of the cell cycle. At the end of S phase, their half-lives drops from 40 min to 10 min. The 3'-UTR of histone mRNA contains a structure made of a 6-bp stem and a 4-nt loop. This element binds a protein that may be responsible for this regulation (Whitfield et al., 2000).

1.5.2. Elements in the coding region

Some elements in the coding region function similarly to those described above. Others interrelate the pathway of translation with the pathway of decay. For example, c-fos mRNA has two coding region determinants (CRD-1 and CRD-2) in addition to an AURE in its 3'-UTR. The CRD-1, located near the center of the RNA body, is the major determinant. It has a 320-nt purine-rich segment that encodes a basic leucine zipper. If CRD-1 is inserted in-frame into β-globin mRNA, it exerts a four-fold destabilization of the mRNA. However, if the insertion is not in-frame, no effect is observed. This sequence interacts with a complex of proteins that includes the p37 isoform of AUF1; NSAP1, which is an hnRNP-like protein; PABP; PAIP-1, which is a PABP-interacting protein; and Unr, which is a purine-rich RNA-binding protein (Grosset et al., 2000). The interaction between CRD-1 and the complex is believed to direct a translation-dependent degradation of the c-fos mRNA, although the mechanism is not fully known.

Microtubules are made of tubulin, a dimer of globular α- and β- subunits. Their assembly are regulated by the cellular concentration of tubulin subunits. The mRNA stability of the β- form, but not that of the α- form, is determined by the initial 13 nucleotides in the coding region. When this element is inserted at the beginning of a reporter gene, the chimeric mRNA becomes responsive to the level of β-tubulin as well.

To function, this element must be placed at the beginning of the coding region and downstream translation is required. There is evidence that the translated four-amino acid sequence is involved in this regulation. Moreover, binding of other factors may also be involved (Bachurski et al., 1994).

1.5.3. Elements in the 5'-UTR

An example of 5'-UTR stability element is the IL-2 mRNA that contains a JNK-response element (JRE) in its 5'-UTR. During T-cell activation, it binds two proteins, nucleolin and YB-1 with high specificity. This binding results in stabilization (Chen et al., 2000). In other examples, stabilization is realized by translation inhibition. Elements that fall into this class usually form a stable stem-loop structure that blocks translation initiation. For reasons that are still unknown, this type of translation inhibition also stabilizes the mRNA (Jacobson et al., 1996).

1.6. Identification of the pH-responsive element

The 955-nt segment (from nucleotides 2009 – 2963) in the 3'-UTR region of GA mRNA was used to initially identify the pH-responsive element. Insertion of this segment enables β-globin mRNA to respond to changes in extracellular pH (Hansen, 1996). Different fragments from this region were inserted downstream to β-globin coding sequence, and the chimeric mRNAs were expressed in LLC-PK_1-F^- cells that were cultured in normal (pH 7.4, 25 mM HCO_3^-) or acidic medium (pH 6.9, 10 mM HCO_3^-). The presence of a pH-responsive element was judged by comparing the stability of the chimeric messenger in the two media. Several of the chimeric constructs exhibited a

faster turnover rate than the β-globin mRNA ($t_{1/2}$ > 30 h) in normal medium and were stabilized when the cells were cultured in acidic medium (Laterza et al., 1997). For example, insertion of the R-2 segment (2344 - 2683) leads to a half-life of 7.8 h in normal medium but a half-life of 30 h in acidic medium. Interestingly, insertion of R-2 in reverse orientation weakened the pH response. This finding suggested the presence of specific element(s) within this region that are responsible for the lability of the GA mRNA under normal conditions and its relative stability during acidic conditions.

RNA gel-shift analyses were performed with this R-2 segment to identify the possible trans-acting element that is involved in the pH response. Kidney cytosolic extract was made from normal rats or from rats that were made acidotic for 18 h. A protein-RNA complex was clearly resolved on a 5% native polyacrylamide gel. Formation of this complex was only effectively competed by addition of excess unlabeled R-2, but not by the adjoining segments of the 955-nt region. Therefore, this complex contains a sequence-specific binding protein that may participate in the pH response pathway.

A deletion experiment was carried out to identify the sequence that contained the protein-binding site. This analysis identified R-2H (76 nucleotide long) and R2-I (29 nucleotide long, located within R-2H) that contained the intact binding site. R-2I is very AU-rich (89.7%), with only three cytosine residues near the two ends. Furthermore, it contains a direct repeat of an eight-base AU sequence in which seven of the eight bases are identical. Mutation of either one of the eight-AU elements to a GC-rich sequence significantly reduced the formation of protein-RNA complex. If both elements were mutated, no protein-RNA complex was formed.

Fig. 1.2. Mapping of the protein binding site within the R-2 RNA.

Panel A. R-2H and R-2I are segments of the 340-base R-2 RNA. R-2H contains 76 bases while R-2I contains 29. The illustrated R-2I RNA sequence is located within R-2H and is highly AU-rich.

Panel B. R-2H and R-2I can form a specific complex with a protein that is contained in a crude cytosolic extract from rat kidney cortex. Both complexes show the same mobility as observed with the R-2 RNA.

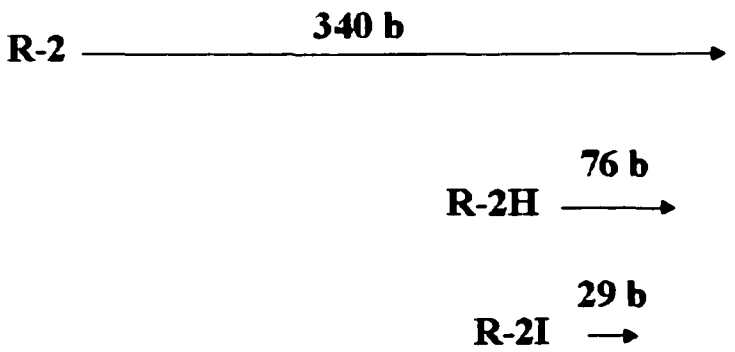

R-2I: UC UUUAAAUA UUAAAAUA AUUACUACUAA

Fig. 1.2A

R-2:	--	+	--	--
R-2H:	--	--	+	--
R-2I:	--	--	--	+

Fig. 1.2B

Attaching the 955 nt 3'-UTR from GA mRNA confers pH-responsiveness to the β-globin mRNA. This chimeric mRNA was mutated so that both of the eight-base AU regions were changed into GC sequences. Such a mutation abolished pH-responsiveness entirely (Fig. 1.3). In another set of experiments, a chimeric mRNA consisting of the β-globin coding region followed by the PEPCK 3'-UTR was expressed in LLC-PK_1-F^- cells. This is a relatively non-responsive mRNA, that exhibits only a one- to three-fold greater half-life in acidic medium compared to in normal medium. However, insertion of a segment containing either one or both of the eight-base AU elements is able to impart a five-fold stabilization to the resulting mRNA (Fig. 1.4). Thus, the AU-elements in the GA 3'-UTR are both necessary and sufficient to function as a pH-responsive element (Laterza et al., 2000).

The apparent binding to R-2I region is increased in cytosolic extracts prepared from the renal cortex of rats that were made acutely acidotic. Similar results were obtained using cytosolic extract prepared from LLC-PK_1-F^- cells that were cultured in acidic medium. Scatchard analysis indicated that the increased binding is due to an increase in both the affinity and the maximal binding of the binding protein (Laterza et al., 2000).

1.7. Regulation of PEPCK during acidosis and its signal pathway.

The increase of PEPCK mRNA level in rat kidney occurs within 1 h after the onset of acute acidosis and reaches a maximum of six-fold at seven h (Hwang et al., 1991). In chronic acidosis, this activation is sustained for up to seven d (Hwang et al., 1991). In contrast to the GA mRNA, its regulation occurs mostly through transcription

Fig. 1.3. Mutation of the AU-rich element in βG-GA mRNA impairs pH-responsiveness.

The AU-rich element was mutated into GC sequence (denoted by XX) to construct pmβG-GA plasmid. This plasmid was used to transfect LLC-PK_1-F^- cells. Stability of this chimeric mRNA was examined for cells cultured in either normal medium (pH 7.4), or in acidic medium (pH 6.9) using northern analysis of total mRNA following DRB treatment.

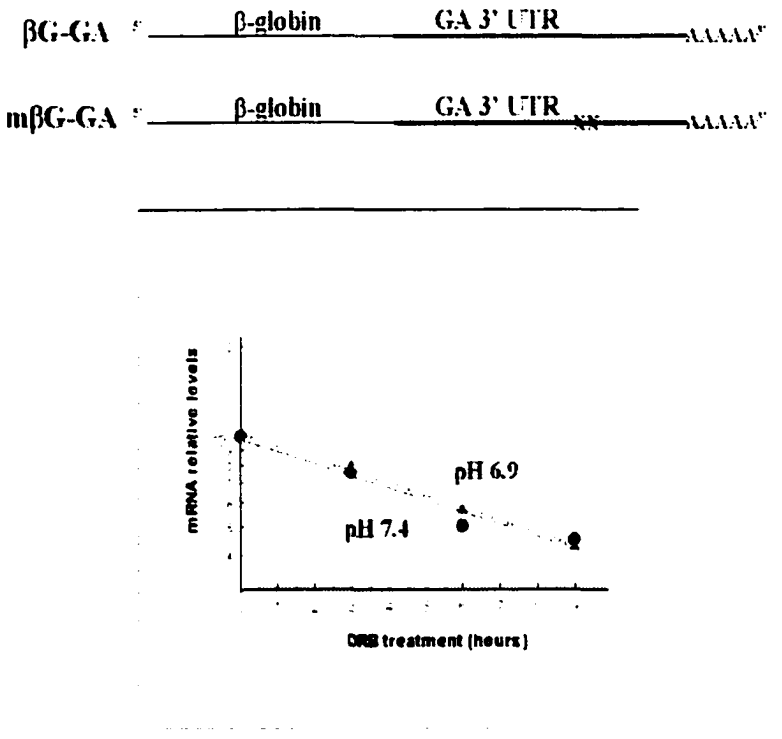

Fig. 1.3

Fig. 1.4. Insertion of the AU-rich element into βG-PEPCK promotes pH-responsiveness.

βG –PEPCK is a less stable mRNA whose pH-responsiveness is not significant. Insertion of R-2H (which contains the AU-rich element) promotes its pH-responsiveness.

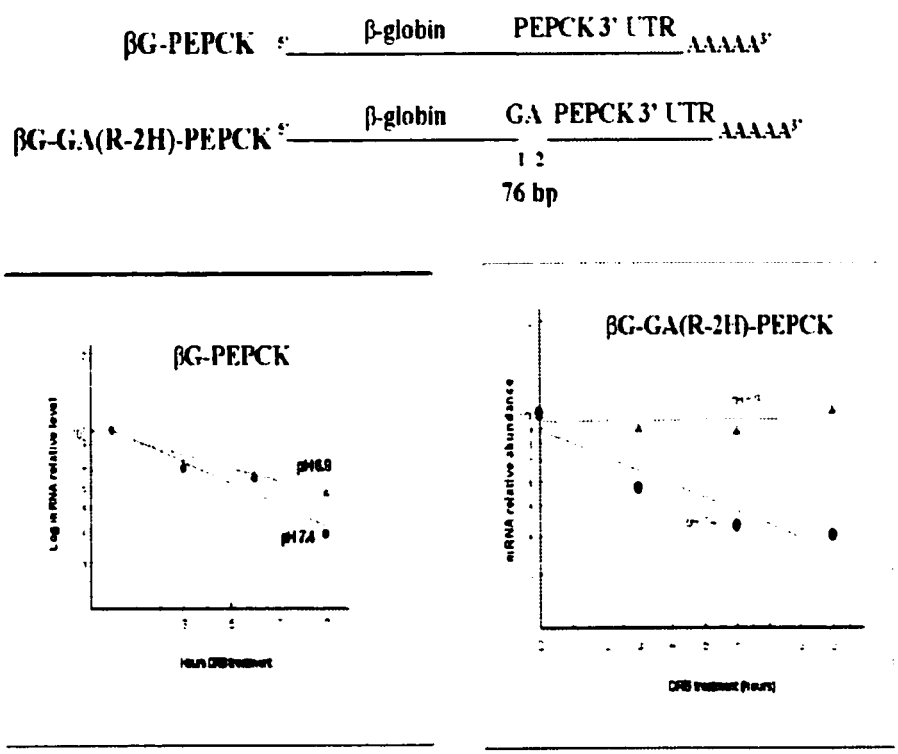

Fig. 1.4

activation. This conclusion was supported by a transcription run-off experiment using isolated rat renal nuclei.

PEPCK promoter region was inserted into the chloramphenicol acetyltransferase (CAT) reporter construct, and the plasmid was used to transfect the LLC-PK_1-F^+ cells when they became confluent and well-differentiated. Within the initial 490-nt promoter region, mutation of the P2 element caused an eight-fold decrease in basal CAT activity, but the activation level that occurred during acidosis was not changed (Holcomb et al., 1995). However, if the P3(II) element, which contains an AP-1 site or the CRE-1 site, were mutated, basal activity was largely unchanged, but the pH-induced activation was reduced. Therefore, some cellular proteins that bind to the P3(II) and the CRE-1 elements may mediate PEPCK mRNA induction during metabolic acidosis. Other studies using longer PEPCK promoter region and cells in subconfluent state confirmed the findings, but also indicated that elements outside the proximal promoter may also be involved (Drewnowska et al., 1997).

Mammalian cells express mitogen-activated protein kinases (MAPKs), which relay extracellular signals inside the cell. At least four groups of MAPKs have been identified. They are extracellular signal-related kinases (ERK1/2), Jun N-terminal kinases (JNK1/2/3), p38 proteins (p38α/β/γ/δ), and ERK5 (Chang et al., 2001). Their signal pathways have a pattern of tiered cascades. MAPKs are activated by upstream protein kinases called MAPK kinases, MAPKKs, MKKs or MEKs, and inactivated by phosphatases. In turn, MAPKKs are activated by further upstream protein kinases called MAPKK kinases, MAPKKKs, or MEKKs, and inactivated by phosphatases. High specificity is often observed, especially at the level of MAPK activation. To summarize,

MEK1/2 are activators for ERK1/2, MKK3/6 for p38, MKK4/7 (JNKK1/2) for the JNKs, and MEK5 for ERK5. Crosstalks may occur at various levels, when one factor can be activated by protein kinases that belong to different group, or when a protein kinase activates multiple substrates.

One function of MAPKs is regulation of transcription. For example, JNKs phosphorylate Jun and activate the transcription of specific genes that contain AP-1 elements (Kallunki et al., 1996). p38 phosphorylates and activates the transcription factor MEF2C (Han et al., 1997). In other cases, MAPKs do not translocate to nuclei. They may exert their influence on post-transcriptional events, targeting cytoplasmic factors. For example, in T cells, JNKs activate a protein that is recruited to the 5'-UTR of IL-2 mRNA and promotes its stabilization (Chen et al., 2000). ERK1/2 phosphorylates carbamoyl phosphate synthetase, a key enzyme in pyrimidines nucleotide synthesis, and thereby regulates DNA synthesis (Graves et al., 2000).

The potential participation of the MAPK pathways in PEPCK mRNA induction was studied by observing the effects of specific MAPK activators and inhibitors on basal or acid-induced expression. Anisomycin, a translation inhibitor and a potent activator of the p38 kinase, increases PEPCK mRNA to levels similar to that observed during acidosis. At the same time, SB203580, a specific p38 inhibitor, blocks PEPCK mRNA induction during acidosis, or the increase caused by anisomycin addition (Feifel, E. et al., submitted to Am. J. Physiol. Renal Physiol). Other inhibitors were also tested. Among them, the ERK1/2 inhibitors, PD098059 and U1236, or the JNK inhibitor, curcumin, had no effect on the basal or induced level of PEPCK mRNA. The above evidence implies that p38 may be involved, while ERK1/2 or JNK are not responsible in this adaptation.

Of the four known p38 isoforms, only the α-isoform is expressed strongly in the LLC-PK_1-F^- cells. ATF-2, a known substrate of p38α, binds to the CRE-1 element of the PEPCK promoter. This was confirmed by gel-shift analysis. ATF-2 antibody was able to supershift some of the complex formed between CRE-1 oligonucleotides and a nuclear extract. Taking all the evidence together, a change in intracellular pH may induce activation of p38/ATF-2 pathway, which further activates PEPCK transcription in the following model (Curthoys et al., 2001): the CRE-1 element in PEPCK promoter is exposed under normal condition. During acidosis, the p38α pathway activates ATF-2, which binds to CRE-1, and initiates an increase in PEPCK transcription.

The p38 kinase is not likely to be involved in the regulation of GA mRNA stability because SB203580 does not block the increase in GA. However, the adaptive changes in PEPCK and GA mRNA levels are coordinately regulated during acidosis. Thus, they may be initiated by the same upstream signal. It will be very interesting to understand how the two distinct responses are mediated.

2. Statement of problem

2. STATEMENT OF PROBLEM

The renal adaptation that occurs during metabolic acidosis includes a series of events. In rat kidney, a significant upregulation of key enzymes in glutamine metabolism is observed. This change, along with the upregulation of various transport proteins, results in an increased renal ammoniagenesis and bicarbonate synthesis, which partially compensate the decreased extracellular pH while preserving the sodium and potassium ion balance.

The first reaction in renal glutamine metabolism is catalyzed by glutaminase. Following the onset of acidosis, glutaminase synthesis is increased to 5.3-fold of its normal level. Concurrently, the level of translatable GA mRNA increases by 4.2-fold. However, the transcription rate of GA gene is largely unchanged during this process. It was determined that a selective stabilization of GA mRNA is responsible for the increased rate of glutaminase synthesis.

The R-2 segment from GA mRNA 3'-UTR was inserted into an expression vector to produce a chimeric mRNA consisting of the β-globin coding region followed by the R-2 sequence. β-globin has been determined to be a very stable mRNA that is non-responsive to changes in medium pH. Insertion of the R-2 segment significantly destabilizes the chimeric mRNA and imparts a pH-responsive stabilization when the cells were transferred to acidic medium.

Using RNA EMSA, a cytosolic protein was found to bind with the R-2 segment. This binding shows a high affinity and specificity. Mapping of the binding site defined a 29-nucleotide AU-rich sequence, possessing a direct repeat of an eight-base AU element.

However, a single element was found to be necessary and sufficient to impart pH-responsiveness.

An affinity purification scheme was designed to take advantage of the high affinity between avidin and biotin. An RNA ligand containing the binding site and two biotinylated nucleotides was synthesized on an ABI synthesizer. This ligand functions as a link to attach the binding protein to an avidin-agarose column. Micro-sequencing was performed to identify the purified protein.

This work identified ζ-crystallin/NADPH:quinone reductase as a protein that participates in the selective regulation of GA mRNA stability during metabolic acidosis. It also provides the reagents necessary to initiate a more detailed characterization of the mechanisms that accomplish the degradation of the GA mRNA and mediate the associated signal transduction pathway.

To further characterize the adaptive stabilization of the GA mRNA during acidosis it was necessary to identify and characterize the protein that binds to the pH-responsive element. Thus, the primary goal of this research was to develop an affinity purification scheme that takes advantage of the high affinity between the pHRE and the binding protein. This was accomplished by testing various biotinylated RNA ligands and utilizing avidin-agarose. The purified protein could be identified by amino acid sequence analysis using tandem mass spectroscopy. Functional studies would then be performed to confirm that the identified protein binds to the pHRE and mediates the pH-responsive stabilization of the GA mRNA.

3. Materials

3.1. MATERIALS

Male Sprague-Dawley rats (140-160 g) were purchased from Charles River. [α-^{32}P]UTP (specific activity 800 Ci/mmol), HRP-conjugated secondary antibody and ECL-Plus kits were obtained from Amersham Pharmacia Biotech. Restriction enzymes, RNase T1, T7 RNA polymerase, and yeast tRNA were acquired from Boehringer Mannheim and New England Biolabs. Biotin-14-CTP was obtained from Gibco. Chemicals for acrylamide gels, Micro Bio-spin chromatography columns, and protein standards were purchased from Bio-Rad. Immobilon NC membrane and Microcon columns were obtained from Millipore. RNasin was obtained from Promega. GelBond PAG films were purchased from Intermountain Scientific. DNA preparation kits were from Promega or Qiagen. Slide-a-lyzer cassettes were obtained from Pierce. Other chemicals were acquired from Sigma. Anti-sera against mouse ζ-crystallin/NADPH: quinone reductase were kindly provided by Dr. J. Samuel Zigler, Jr. (National Eye Institute). A monoclonal antibody against the mouse T-cell restricted intracellular antigen-related protein, TIAR was kindly provided by Dr. Nancy Kedersha (Harvard Medical School).

3.2. BUFFERS AND SOLUTIONS

Krebs-Henseleit Saline buffer (KHS)

118 mM Sodium Chloride

4.8 mM Potassium Chloride

1.2 mM Sodium Phosphate

1.2 mM Magnesium Phosphate

2.5 mM Calcium Chloride

25 mM Sodium Bicarbonate

5.5 mM Glucose

1.0 mM Acetoacetate

1.0 mM Alanine

0.1 mM Myoinositol

2.0 mM Glutamine

pH to 7.4

Rat Renal Cortex Cytoplasmic Extraction Buffer

40 mM Hepes

100 mM Potassium Acetate

10 mM Magnesium Acetate

1 mM Dithiothreitol

0.01 mM Leupeptin

0.01 mM Antipain

5 µg/ml Phenylmethylsulfonylfluoride

pH 7.4

10X *In vitro* Transcription Buffer (from Promega):

200 mM Tris-HCl, pH 7.9

30 mM Magnesium Chloride

10 mM Spermidine

50 mM Sodium Chloride

DEPC-treated water

0.1% (v/v) Diethyl pyrocarbonate

37 °C overnight and autoclaved

10X MOPS buffer

0.2 M MOPS

10 mM Sodium Acetate

10 mM EDTA

RNA agarose gel running buffer

35 ml 10X MOPS

28 ml Formaldehyde (37% v/v)

287 ml H_2O to make a total of 350 ml

5X TBE buffer

450 mM Tris, pH 8.2

550 mM Boric Acid

10 mM EDTA

50X TAE buffer

2.0 M Tris-acetate, pH 8.0

100 mM EDTA

Water-saturated phenol

0.1% 8-Hydroxyquinoline (v/v) and thoroughly mixed with an equal volume of deionized water

1X Dialysis buffer

10 mM Hepes

25 mM Potassium Acetate

2.5 mM Magnesium Acetate

1 mM Dithiothreitol

pH to 7.4

Lower Tris Stock

18.17 g Tris base

4 ml 10% SDS

pH 8.6

adjust to 100 ml

Upper Tris stock

6.06 g Tris base

4 ml 10% SDS

pH 6.6

adjust to 100 ml

Sample buffer

10 ml Glycerol

5 ml β-Mercaptoethanol

30 ml 10% SDS

12.5 ml Upper tris stock

5 ml 0.05% Bromophenol blue

adjust to 100 ml

Reservoir buffer stock

12 g Tris base

57.6 g Glycine

pH 8.5

adjust to 1000 ml

NEPHGE tube gel

1.141 g Urea

500 µl 30% Acrylamide

600 µl 10% NP-40

400 µl Water

188 µl 2-D Pharmalytes

Lysis buffer

9.5 M Urea

2% NP-40

2% Pharmalytes

5% 2-Mercaptoethanol

store aliquots at –70 °C

Overlay solution

9.0 M Urea

1% Pharmalyte

store aliquots at –70 °C

2-D agarose

1g Agarose

12.5 ml 1M Tris

85.6 ml Water

1 ml 10% SDS

pH 6.8, adjust to 100 ml

Equilibration buffer

0.5 ml 10% SDS

6.25 ml 1 M Tris

5 ml 2-Mercaptoethanol

5 ml 0.05% Bromophenol blue

pH 6.8, adjust to 50 ml

4. Methods

4. METHODS

4.1. Cytosolic extract preparation from rat kidney

Rats were made acidotic by stomach loading with 20 mmol of NH_4Cl/kg body weight and then providing 0.28 mM NH_4Cl as the sole source of drinking water. After 18-24 h, the rats were anesthetized with 1 mg/kg body weight of pentobarbital and opened with a midline incision. The kidneys were perfused *in situ* with Krebs-Henseleit solution and then removed, decapsulated, sliced longitudinally, and placed in ice-cold Krebs-Henseleit solution. The cortex was dissected free of papilla and medulla and then cut into small pieces. The cortical tissue was placed in an equal volume of cytoplasmic extraction buffer and disrupted with a Dounce homogenizer. The homogenate was centrifuged for 10 min at 1,000X g to pellet intact cells and nuclei. The supernatant was centrifuged at 10,000X g for 10 min to pellet the mitochondria and then for 90 min at 100,000X g to pellet membrane-bound organelles and polyribosomes. The final supernatant was divided into 100-µl aliquots and stored frozen at -70 °C. The protein concentration of the cytosolic extract was determined by a Bradford assay (Bradford, 1976) using bovine serum albumin as the standard.

4.2. Cytosolic extract preparation from LLC-PK_1-F^+ cells

A 10-cm plate of cultured cells was thoroughly washed with ice-cold Krebs-Henseleit solution. The cells were then mixed with 100 µl of cytoplasmic extraction buffer. Cells were disrupted with a micro-Dounce homogenizer and centrifuged for 10 min at 1,000X g to pellet intact cells and nuclei. The supernatant was centrifuged at

10.000X g for 10 min to pellet the mitochondria and then at 100.000X g for 90 min to pellet membrane-bound organelles and polyribosomes. Supernatant was aliquoted and saved at –70 °C. Protein concentration was determined by a Bradford assay (Bradford, 1976), with bovine serum albumin as standard.

4.3. Dialysis

Sample was carefully injected into a Slide-A-Lyser cassette and then dialyzed overnight at 4 °C against 5000 volumes of prechilled 1X binding buffer.

4.4. DNA template isolation for *in vitro* transcription

The cDNA sequences that encode the R-2I, R-2H, mut1, mut2, mut3 and $A(UUUA)_5$ RNAs were cloned into pBlueScript II-SK(-)downstream to the T7 promoter (Laterza et al., 1997). The DNA templates were isolated by digesting the respective plasmids at the *BSSH II* site that is immediately upstream of the T7 promoter, and a restriction enzyme site that is downstream to the inserted sequence. The R-2H plasmid was digested with *BSSH II* and *Hind III* to produce the template for synthesis of the 113 base R-2H RNA. The other plasmids were digested with *BSSH II*, *Sal I*, and *Xba I*. The short DNA templates were purified using an 8% to 12% polyacrylamide gel and extracted using the "crush and soak" procedure (Sambrook et al., 1989). The final concentrations ranged from 0.2-1.0 mg/ml.

4.5. *In vitro* transcription

The isolated templates were transcribed in a 10-µl reaction mixture containing the following components: 100 ng of template DNA, 20 µCi [α-^{32}P]UTP, 0.5 mM ATP, CTP and GTP, 50 µM unlabeled UTP, 20 units of RNAsin, 1 µl T7 polymerase and 10 mM dithiothreitol. After incubating at 37 °C for 1 h, 1.0 unit of RNase free-DNase was added and the reaction mixture was incubated at 37 °C for 15 min. The RNA was then purified by chromatography on a Micro Bio-spin column and its concentration was determined by scintillation counting.

Syntheses of unlabeled RNAs were performed using 100-µl of the same reaction mixture but lacking [α-^{32}P]UTP and containing a 0.5 mM concentration of each ribonucleotide. The concentrations of the purified RNA samples were determined by measuring their absorbance at 260 nm and using specific extinction coefficients calculated from the nucleotide composition of the individual transcripts.

4.6. RNA agarose gel

A 2% gel was prepared by dissolving 1 g of agarose in 36 ml of boiling water. After cooling to 55 °C, 5 ml of 10X MOPS and 9 ml of formaldehyde (37% v/v) were added, and the solution was poured into a gel apparatus. Samples were prepared by adding 1 µl of RNA, 5 µl of deionized formamide, 2 µl of formaldehyde and 2 µl 10X MOPS buffer. Ethidium bromide (0.6 pg) was added and the samples were heated for 10 min at 65 °C, followed by cooling on ice for 10 min. Approximately 50 ng of bromophenol blue was added as indicator during electrophoresis.

4.7. RNA EMSA

Either 3 μg of a rat renal cortical extract or 10-50 ng of purified protein were preincubated for 10 min at room temperature in a 10-μl reaction mixture containing 10 mM Hepes, pH 7.4, 25 mM potassium acetate, 2.5 mM magnesium acetate, 0.5 μg of yeast tRNA, 0.5% Igepal CA 630, 5% glycerol, 1 mM dithiothreitol, and 10 units of RNAsin. Where indicated, specific antibodies were added and the mixture was incubated for 20 min at room temperature. Subsequently, 20 fmol of labeled R-2I RNA was added. For competition experiments, specific or non-specific competitors (100-fold excess) were also added. The samples were incubated for 20 min at room temperature and then subjected to electrophoresis for 90 min in a 5% polyacrylamide gel at 170 V using a 90 mM Tris, 110 mM boric acid, 2 mM EDTA running buffer. The gels were dried and imaged using a PhosphorImager screen.

4.8. Synthesis of purification ligand

The following oligonucleotide was synthesized by Macromolecular Resources (Ft. Collins, CO):

$^{5'}$TTAGUGUGACUCUUUAAAUAUUAAAAUAAUUACUACUAACUGUUCATTdA TTT$^{3'}$. The 5'-end contained two deoxythymidines and the 3'-end contained six deoxyribonucleotides including two biotinylated thymidines (Glen Research, Sterling, VA, indicated in bold). The remainder of the oligonucleotide was composed of a sequence of ribonucleotides derived from the GA mRNA. The underlined nucleotides are

the direct repeat of the eight-base AU-sequence that constitutes the pH-response element of the GA mRNA.

4.9. Purification with FPLC

A 1-ml sample of a rat renal cortical cytosolic extract (~ 20 mg of total protein) was dialyzed overnight against 1X binding buffer containing 10 mM Hepes, pH 7.4, 25 mM potassium acetate, 2.5 mM magnesium acetate and 1 mM dithiothreitol. The following additions were made to the dialyzed extract: 40 µl 10% Igepal CA 630, 1 mg tRNA, 20 µmol dithiothreitol and 20 µl RNAsin (40 units/µl). The sample was then incubated at 4 °C for 10 min. The biotinylated RNA ligand was centrifuged through a Micro Bio-spin P6 column. Approximately 2 nmol of the purified ligand were added and the mixture was incubated at 4 °C for an additional 20 min. An FPLC column was packed with 0.5 ml of avidin agarose (10-fold excess with respect to the biotinylated RNA) and washed extensively with 1X binding buffer. The complete sample was loaded onto the column at a flow rate of 0.1 ml/min. The column was then eluted with a gradient of increasing ionic strength at a flow rate of 0.05 ml/min. To produce the gradient, the concentrations of the potassium acetate and magnesium acetate in the 1X binding buffer were increased proportionately. The collected fractions (0.5 ml) were dialyzed versus 1X binding buffer and assayed by RNA gel shift analysis. To assess purity, samples from the collected fractions containing 10 ng of protein were separated on a 10% polyacrylamide gel containing 1% SDS and stained with 0.1% silver nitrate.

4.10. Protein precipitation

To a 150 µl aliquot of protein, 600 µl methanol, 150 µl chloroform and 450 µl water were added in the specified order. The tube was vortexed after each addition. It was then spun at 14,000 X g for 5 min and the upper phase was removed without disturbing the interphase. The protein was precipitated from the interphase by adding 450 µl methanol, vortexing and centrifuging at 14,000 X g for 5 min. The supernatant was removed carefully and the tube was dried thoroughly. The protein pellet was later dissolved in 1X binding buffer.

4.11. Sample preparation for trypsin digestion and sequencing

The electrophoresis unit and all glassware were incubated overnight with 2% cleansing concentrate (Bio-Rad), followed by extensive washing with doubly deionized H_2O. The purified protein was concentrated, subjected to SDS-PAGE and stained with freshly prepared Coomassie Blue. The 36-kDa protein band was excised, sealed in an Eppendorf tube and sent to the Harvard Microchemistry Facility (Dr. William S. Lane) for analysis. The protein was subjected to in-gel reduction, carboxyamidomethylation, and tryptic digestion. Multiple peptide sequences were determined by microcapillary reverse-phase chromatography coupled to a Finnigan LCQ quadrupole ion trap mass spectrometer. Interpretation of the resulting MS/MS spectra was facilitated by software developed in the Harvard Microchemistry Facility and by data base correlation with the algorithm SEQUEST.

4.12. Western analysis

The proteins contained in 150-μl samples of the individual column fractions were concentrated by chloroform/methanol precipitation and washed with methanol. The protein pellets were then resuspended in Laemmli sample buffer. The samples were separated by SDS-PAGE using a 10% separating gel, transferred to a nitrocellulose membrane, and incubated with either a 1:500 dilution of ζ-crystallin/NADPH:quinone reductase antiserum or with a 1:2000 dilution of TIAR monoclonal antibody. The membrane was then incubated with a 1:1500 dilution of HRP-conjugated secondary antibody. Images were developed with ECL-Plus kit and visualized on a Storm Instrument (Molecular Dynamics).

4.13. 2-D electrophoresis

Non-equilibrium pH gradient electrophoresis (NepHGE) was used in the first dimension. Ampholyte (pH 3-10) was used to make tube gels that are 75 mm in length, and 1.2 mm in diameter. Protein was precipitated and dissolved with the least possible amount of 9.0 M urea. A 20 mM phosphoric acid solution was as the anolyte, whereas a 50 mM sodium hydroxide solution was used as the catholyte. Separation was carried out using 1200 V as the maximum voltage and 0.1 watt/tube as the maximum power. Sample and control tubes (used to determine pH values at both ends) were run for 2 h.

The tube gel was then carefully removed without confusing its ends. A 10% SDS-PAGE was used on the second dimension. Protein was visualized using silver staining.

4.14. Construction of ζ-crystallin bacterial expression vector

A *BSSH II* fragment of pMLR107 that contains a full-length cDNA of mouse ζ-crystallin was used as the template for a PCR reaction. The following two primers were synthesized to amplify the entire coding sequence, while introducing an *Nde I* site at the 5` end and a *Bgl II* site at the 3` end (indicated in bold).

1. GC**CATATG**GCAACTGGGCAGAAGTTGATGAGG
2. CCTCTTATGAGACCTGTGTCACTGGGC**AGATCT**CG

The *Nde I/Bgl II* fragment of the PCR product was inserted into the pET-3a or pET-15b vector (which has a hisX6 tag) at their *Nde I* and *BamH I* sites. (*BamH I* and *Bgl II* have compatible overhanging sequences.) The resulting plasmids (Fig. 4.1A and B) express ζ-crystallin coding region from a T7 promoter.

Both vectors were verified with restrictive digestion and sequencing from both ends of the inserted segment.

4.15. construction of ζ-crystallin eukaryotic expression vector

An *Xba I/Dra I* fragment of pMLR107, which includes the full length coding region of ζ-crystallin was inserted into pcDNA3.1 vector at its *Nhe I* and *EcoR V* sites. (*Xba I* and *Nhe I* generate compatible ends while *Dra I* and *EcoR V* generate blunt ends.) (Fig. 4.2) The resulting plasmid was verified by restrictive digestion and sequencing from both ends of the inserted segment.

Fig. 4.1. Construction of ζ-crystallin vector for expression in E. coli DE3 cells.

Panel A. Construction of pET-3a-zeta vector. The *Nde I/Bgl II* fragment of the PCR product (containing the coding region of ζ-crystallin) was inserted into the *Nde I* and *BamH I* sites of pET-3a.

Panel B. Construction of pET-15b-zeta vector. The *Nde I/Bgl II* fragment of the PCR product (containing the coding region of ζ-crystallin) was inserted into the *Nde I* and *BamH I* sites of pET-15b.

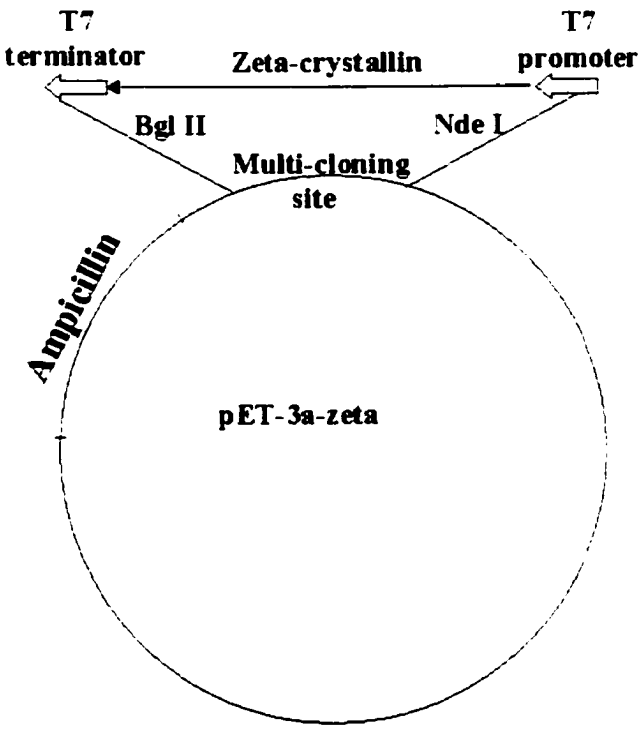

Fig. 4.1A

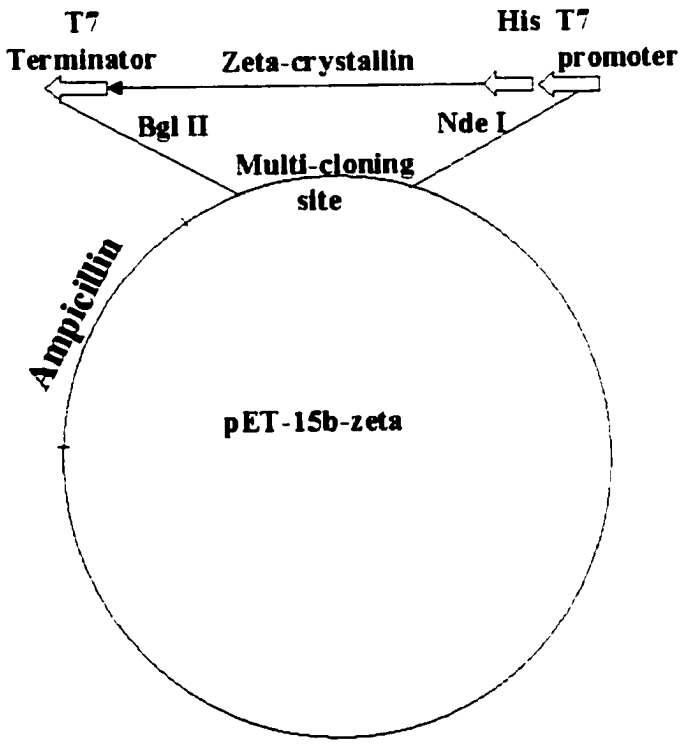

Fig. 4.1B

Fig. 4.2. Construction of ζ-crystallin vector for expression in LLC-PK$_1$-F$^-$ cells.

An *Xba I/Dra I* fragment from PCR-zeta plasmid (containing the coding region of ζ-crystallin) was inserted into the *Nhe I* and *EcoR V* sites of pcDNA3.1.

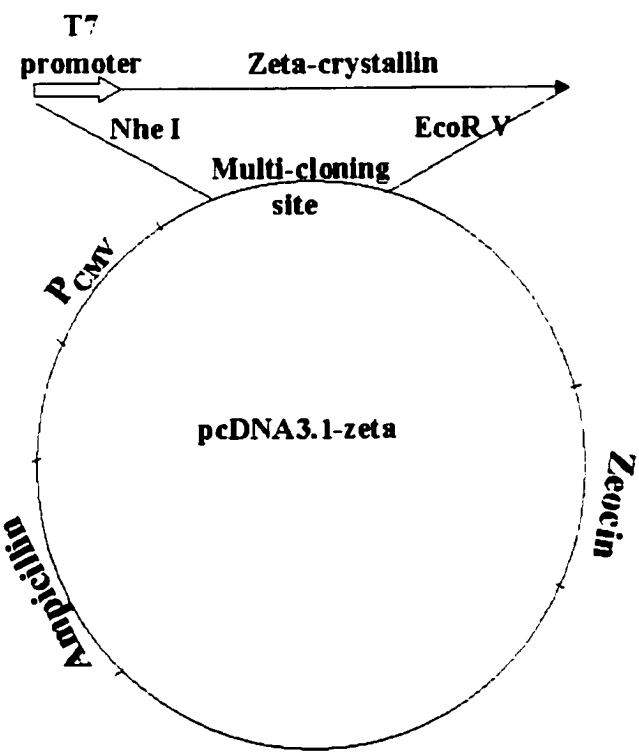

Fig. 4.2

5. Results

5. RESULTS

5.1. Purification of pHRE-BP with ligand transcribed *in vitro*

5.1.1. *in vitro* transcription of biotinylated ligand

The *in vitro* transcription protocol was modified so that some of the CTP was replaced with an equal amount of biotin-CTP. The resulting RNA was applied to an RNA agarose gel and its mobility was compared to that of RNA prepared without biotin-CTP. The biotin-CTP contained biotin attached to the N4 position of CTP via a 14-atom linker. The T7 polymerase effectively incorporates biotin-CTP into RNA in place of cytosine. However, because of the additional mass of the biotin group, the biotinylated RNAs were expected to migrate more slowly in an RNA agarose gel.

Initially, the R-2H RNA was transcribed using reaction mixtures that contained different ratios of CTP and biotin-CTP, and the resulting products were analyzed on a 2% agarose gel. A 1:1 mixture of biotin-CTP and CTP did not produce satisfactory biotinylation (Fig. 5.1A). This was not surprising, because T7 polymerase was known to have a lower preference for the biotin-CTP. Biotinylation was improved by using a 9:1 mixture of biotin-CTP and CTP (Fig. 5.1B).

Transcription of the R-2I RNA was carried out using 9:1 and 29:1 ratios of biotin-CTP and CTP (Fig. 5.1C). Both reaction mixtures produced a biotinylated product.

From a 10 µl reaction, 2.3 µg of R-2I RNA were obtained with the 9:1 ratio and 1.2 µg of R-2I RNA were generated with the 29:1 ratio. Thus, in the following experiments, unless specified otherwise, the 9:1 ratio was used.

Fig. 5.1. In vitro transcription of biotinylated RNAs

Panel A. R-2H RNA was synthesized by *in vitro* transcription. In reaction 1, equal amounts of the four nucleotides were used. In reaction 2, half of the CTP was replaced with biotin-CTP. The RNA products were resolved on a 2% RNA agarose gel.

Panel B. In reaction 2, 90% of the CTP was replaced with biotin-CTP.

Panel C. R-2I RNA was synthesized by *in vitro* transcription. In reaction 1, equal amounts of the four nucleotides were used. In reaction 2, 90% of the CTP was replaced with biotin-CTP. In reaction 3, 97% of the CTP was replaced with biotin-CTP. The RNA products were resolved on a 2% RNA agarose gel.

Fig. 5.1A

Fig. 5.1B

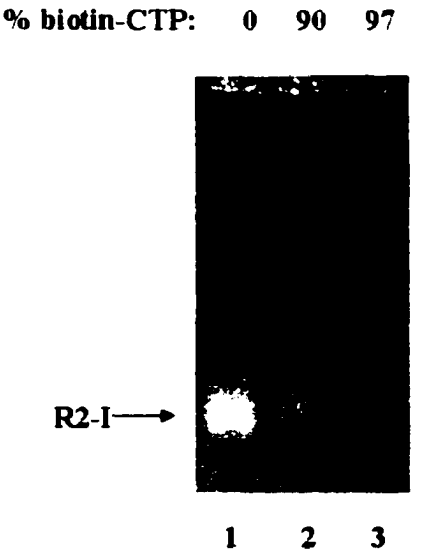

Fig. 5.1C

5.1.2. Binding assay of biotinylated RNA

The R-2I RNA contains three cytosine residues that are located at the 3`-end far from the AU-element. For this reason, we projected that incorporation of biotin-CTP should not affect binding to the pHRE-BP. In order to verify this, an RNA EMSA was performed (Fig. 5.2) using the biotinylated R-2I RNA and a crude extract from rat kidney cytosol. The resulting protein-RNA complex exhibited a mobility similar to that observed with the non-biotinylated R-2I RNA. The two probes also produced shifted bands of comparable intensity, indicating that incorporation of biotin-CTP did not affect the binding affinity between the probe and the pHRE-BP.

An experiment was performed to determine the optimal incubation time for the pHRE-BP contained in a crude extract to interact with the RNA probe. The incubation should be sufficient to maximize complex formation without causing significant RNA degradation. With both non-biotinylated and biotinylated R-2I RNA, the amount of protein-RNA complex was increased only slightly in incubations that were greater than 5 min (Fig. 5.3). However, incubations up to 60 min produced very little degradation.

Before attempting a large-scale purification, an experiment was performed to determine the minimum amount of RNAsin required to prevent degradation of the biotinylated RNA. As shown in Fig. 5.4, a concentration of RNAsin below 0.4 unit/μl was insufficient to prevent the RNA from being degraded. Thus, a concentration greater than this level was required.

Fig. 5.2. Comparison of the binding interaction of biotinylated and non-biotinylated R-2I RNA with pHRE-BP.

Biotinylated (lanes 1 & 3) and non-biotinylated (lanes 2 & 4) R-2I RNAs were synthesized by *in vitro* transcription using [α-^{32}P]-UTP. The labeled transcripts (25 fmol) were incubated with (lanes 3 & 4) or without (lanes 1 & 2) 3 μg of a crude cytosolic extract from rat kidney cortex. The protein-R-2I complexes were resolved on a native 5% polyacrylamide gel.

RNA biotinylation:	--	+	--	+
Crude extract:	--	--	+	+

← **Protein-R2-I complex**

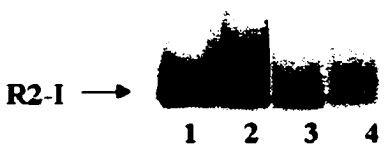

Fig. 5.2

Fig. 5.3. Effect of incubation time on protein R-2I complex formation.

Biotinylated R-2I RNA (25 fmol) was incubated with 3 μg of a crude rat kidney extract on ice for 5, 20 or 60 min. As a control, non-biotinylated R-2I RNA (25 fmol) was used. The protein-R-2I complexes were resolved on a native 5% polyacrylamide gel.

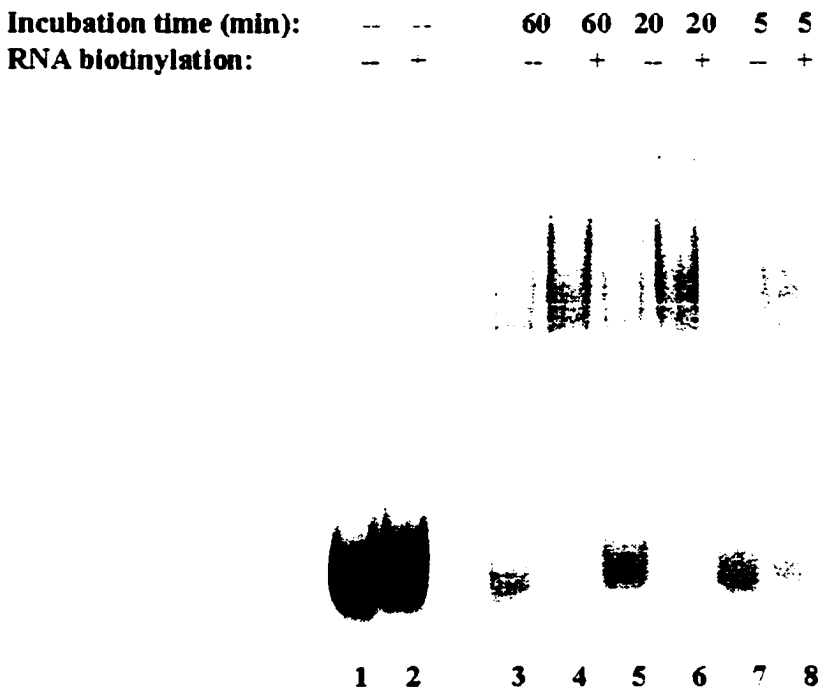

Fig. 5.3

Fig. 5.4. Effect of RNAsin concentrations on protein-R-2I complex formation.

Biotinylated R-2I RNA (25 fmol) was incubated with 3 μg of a crude rat kidney extract for 5, 20 or 60 minutes on ice. The RNAsin concentration was varied (0.04, 0.13, 0.4 unit/μl). The protein-R-2I complexes were resolved on a native 5% polyacrylamide gel.

Incubation time (min):	**60**	**60**	**60**	**20**	**20**	**20**	**5**	**5**	**5**
RNAsin concentration (unit/μl):	**.04**	**.13**	**.4**	**.04**	**.13**	**.4**	**.04**	**.13**	**.4**

Fig. 5.4

5.1.3. Purification with the biotinylated R-2I

A small-scale purification was performed with 30 µl of crude extract of rat kidney cortex containing 25 µg/µl protein. Using an estimated abundance of 0.05% and a protein mass of 48 kDa, the amount of pHRE-BP was estimated to be:

30 µl * 25 µg/µl * 10^{-6} * 0.05% / 48,000 g/mol = 7.8 pmol

The extract was incubated at room temperature for 10 min with the appropriate amounts of tRNA, dithiothreitol, and RNAsin, whose amounts were all scaled up from the RNA EMSA incubation mixture.

Then 1 µl containing 0.46 µg of biotinylated R-2I (52 pmol) was added and the sample were incubated at room temperature for 20 min. The moles of biotinylated RNA was estimated using the length of R-2I (29 nt) and 330 as the average molecular mass of a nucleotide:

0.46 µg * 10^{-6} / (29 * 330 g/mol) = 52 pmol of R-2I.

Thus, the amount of added RNA was about 6 fold greater than the estimated amount of pHRE-BP.

Then, 50 µl of avidin agarose were added. This aliquot contained more than a 10-fold excess of biotin-binding sites than contained in the R-2I RNA, even if all 3 cytosines had incorporated biotin-CTP. This mixture was incubated with gentle shaking at room temperature for 30 min.

The mixture was applied to a column containing a porous support to retain the agarose beads. The column was then washed with five 200-µl aliquots of 1X binding

buffer. Each flow-through was collected as a separate sample and labeled W1 through W5. Then, a 2 M KCl solution was applied to the column, and two 100-µl fractions were collected. Eluants were labeled E1 and E2.

The W1, W2 and E1 samples were dialyzed against 1X binding buffer and their binding ability was compared with that of crude extract (Fig. 5.5). The E1 sample failed to form complex with the R-2I RNA. The observed distortion in this lane suggests that this fraction was not completely dialyzed. Thus the residual salt may have prevented binding. However, significant binding activity was observed with the W1 and W2 samples. Considering the respective sample volumes, it was more likely that the pHRE-BP was eluted before the high salt solution was applied. This result was unexpected, because the pHRE-BP should have remained bound to R-2I RNA when the column was washed with 1X binding buffer.

5.1.4. Purification with biotinylated R-2H

It was assumed without examination that the biotinylated R-2I binds effectively to avidin agarose. To address this assumption, the following experiment was performed (Table 5.1). Biotinylated R-2I and R-2H RNAs were synthesized using [α-^{32}P]-UTP. After purification, the labeled probes were incubated with an excess of crude extract. As a control, no crude extract was added. Then, an excess of avidin agarose was added and gently mixed. The supernatant was isolated by centrifuging the tube, and its radioactivity was measured by scintillation counting. The level of radioactivity remaining in the supernatant represented the RNA that did not bind to the agarose matrix (Table 5.1).

Fig. 5.5. Binding activity recovered in various fractions from a small-scale purification of the pHRE-BP using a biotinylated R-2I ligand.

A small-scale purification was performed using biotinylated R-2I RNA as the ligand. Fractions containing the proteins recovered with two aliquots of wash buffer (W1 and W2) and one aliquot of elution buffer (E1) were dialyzed and analyzed by RNA-EMSA using an equal volume (7 µl) of each sample. The protein-R-2I complexes were resolved on a native 5% polyacrylamide gel.

Crude extract:	--	+	--	--	--
Fractions from purification:	--	--	**W1**	**W2**	**E1**

Fig. 5.5

Table 5.1. Binding efficiency of two probes to avidin agarose.

Either 0.5 pmol of biotinylated R-2I RNA or 0.3 pmol of biotinylated R-2H RNA was used in each reaction. In reactions 2 and 4, RNA probes were incubated with 5 µl rat kidney cytosolic extract (containing ~1 pmol pHRE-BP) followed by incubation with avidin agarose. No extract was added in reactions 1 or 3. Radiation levels were measured on the scintillation counter.

Reaction	probe	Total counts (cpm)	Cytosolic extract	Supernatant counts (cpm)	% bound
1	Biotinylated R-2I	$9.5*10^4$	No	$6.9*10^4$	27
2	Biotinylated R-2I	$9.5*10^4$	Yes	$7.0*10^4$	26
3	Biotinylated R-2H	$1.4*10^5$	No	$8.3*10^3$	94
4	Biotinylated R-2H	$1.4*10^5$	Yes	$2.0*10^4$	86

Table 5.1

Most of the radioactivity for the R-2I RNA remained in the supernatant. This meant that much of the biotinylated RNA did not bind to avidin agarose, which was recovered in the pellet. The presence or absence of cell extract did not make a significant difference. Therefore the failure of the R-2I RNA to bind to avidin must be due to the non-accessibility of its biotinylated sites. In contrast, a large percentage of the labeled R-2H RNA did bind to the avidin agarose. Addition of crude extract decreased the binding only slightly (from 94% to 86%). The greater binding could be explained by the availability of more biotinylation sites within the R-2H RNA. In other words, while the R-2I RNA bound well to the pHRE-BP, the incorporated biotin was not accessible to the avidin agarose.

Thus, the small-scale purification was repeated with biotinylated R-2H RNA and 10 µl of crude extract. Five rounds of washing (W1-W5) were done with the following volumes: W1: 40 µl, W2-W5: 200 µl. Two rounds of elution were done with 100 µl aliquots of 2 M KCl. The binding activity of the recovered samples was compared to that of the crude extract (Fig. 5.6). Much of the binding activity was recovered in the first two washes, but some binding activity did remain bound through the wash steps and was eluted with the 2 M KCl solution.

With 6 µl of E1, 5% R-2I RNA formed a protein-RNA complex. This was 10% of the binding activity observed with 1/6 µl of crude extract. Therefore the purification efficiency was estimated as below:

10% / 6 µl * 100 µl * 1/6 µl / 10 µl = 3%

Fig. 5.6. Binding activity recovered in various fractions from a small-scale purification of the pHRE-BP using a biotinylated R-2H ligand.

A small-scale purification was performed using biotinylated R-2H RNA as the ligand. Fractions recovered from five rounds of washing (W1 through W5) and from two rounds of elution (E1 and E2) were dialyzed. A 1-µl sample of fraction W1 (lane 3) and 6-µl samples of the all other fractions (lanes 4 – 10) were incubated with 25 fmol of [^{32}P] labeled R-2I RNA. The protein-R-2I complexes were resolved on a native 5% polyacrylamide gel.

Crude extract:	–	+	–	–	–	–	–	–	–	–
Fractions from purification:	–	–	**W1**	**W1**	**W2**	**W3**	**W4**	**W5**	**E1**	**E2**

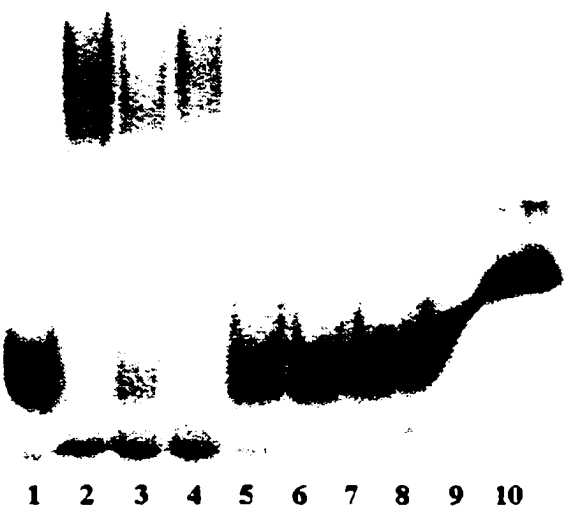

Fig. 5.6

It is possible that some of the binding activity was denatured by the high salt concentration used in the purification. Therefore the actual efficiency could be higher.

5.2. Synthesis of purification ligand

Various RNA binding proteins have been purified using a biotinylated RNA ligand that was generated through organic synthesis (Rouault et al., 1989 and Ross et al., 1997). The advantages of this approach are as follows:

1. The ligand can be produced in large amount. In contrast, multiple transcription reactions would be needed to purify enough protein for sequencing.

2. The accuracy and purity of the synthesized oligonucleotide was assured, as was indicated by mass spectroscopic analysis. Synthesized RNA was aliquoted into small fractions to ensure reproducible RNA quality.

3. In *in vitro* transcription, biotin-CTP was incorporated randomly by T7 polymerase. Thus, the resulting product is heterogeneous with regard to location and number of biotinylation sites. The various products could bind to avidin agarose and the pHRE-BP with different affinities. In contrast, with the synthesized RNA ligand the location of biotinylation sites was defined and homogeneous.

4. Deoxyribonucleotides could be added at both ends of the RNA to prevent degradation by exoribonucleases.

An RNA ligand (shown in Method section) was synthesized to contain the putative protein recognition site (Fig. 5.7). The 5' and 3' flanking ends were designed to be longer than the R-2I RNA to ensure enough space to allow for avidin-biotin

Fig. 5.7. Comparison of the RNAs used for gel-shift assays and as a ligand for affinity purification.

All three RNAs contain the direct repeat of two eight-nucleotide AU-sequences that constitute the pHRE from the GA mRNA. In total the R-2I and R-2H RNAs contain 29 and 72 nucleotides, respectively. The affinity ligand contained 44 ribonucleotides and the indicated deoxyribonucleotides (italic) including two biotinylated thymidines.

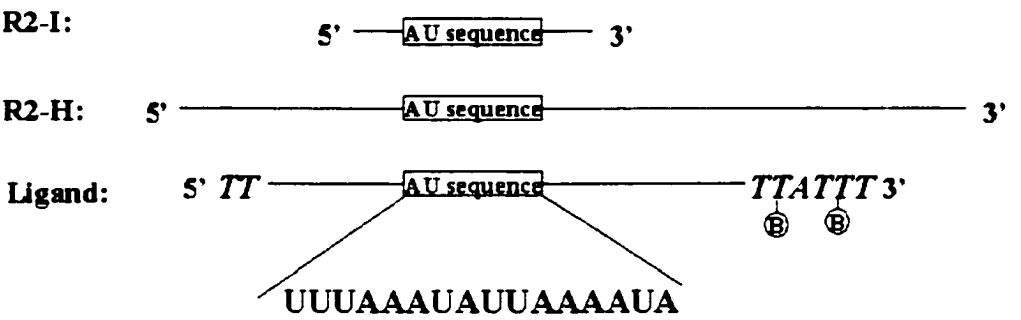

Fig. 5.7

interaction. They were shorter than R-2H to avoid non-specific binding as much as possible and to minimize cost.

The synthesized RNA ligand was aliquoted and dried in a SpeedVac.

5.3. Purification of pHRE-BP with synthesized ligand.

5.3.1. Elution profile.

An FPLC was used in the purification protocol to purify the RNA-binding protein in order to reproducibly generate the desired gradient and to control flow rate. Similar to previous purifications, a crude cytosolic extract from rat kidney cortex was incubated with the RNA ligand under optimal binding conditions. It was feasible to use lower amounts of RNAsin due to the protected structure of the RNA ligand.

Washing with 1X binding buffer should not elute the pHRE-BP protein. However, it was not sufficient to effectively remove all proteins that bind non-specifically. As is shown in Fig. 5.8A, after an extensive wash of 30 ml 1X binding buffer, a large number of proteins were eluted as the salt concentration of the elution buffer was gradually increased. Similar result was observed using a step-wise gradient. (Fig. 5.8B)

Fractions that correspond to the protein peak in Fig. 5.8A were analyzed on a 10% SDS PAGE. They contained a heterogeneous mixture of many different proteins.

5.3.2. Salt gradient for FPLC and purified protein.

After many trial-and-error attempts, an effective wash and elution profile was developed (shown in Fig. 5.9). The cytosolic extract from rat kidney cortex was

incubated with a sufficient excess of the affinity ligand to saturate all of the pHRE-BP. The resulting complex was then applied to an FPLC column that had been packed with avidin-agarose and equilibrated with the 1X binding buffer. The column was washed extensively with 1X binding buffer and then eluted by increasing proportionately the concentrations of potassium acetate and magnesium acetate according to the gradient profile. The pH and concentrations of HEPES and DTT were kept constant. The eluant through the wash with 4X binding buffer (100 mM potassium acetate and 10 mM magnesium acetate) contained very little R-2I RNA binding activity. Thus, 0.5-ml fractions were routinely collected only as the steep gradient of 4X to 20X binding buffer was applied to the column. An aliquot of each fraction was analyzed by SDS-PAGE and silver staining. As shown in Fig. 5.10A, two proteins were recovered in these fractions. The elution of a 43-kDa protein peaked in fraction 4 and a 36-kDa protein peaked in fraction 7. When larger volumes of the peak fractions were concentrated by chloroform/methanol precipitation and subjected to SDS-PAGE, additional protein bands with varying sizes were observed. However, the additional proteins constituted less than 5% of the total protein (data not shown).

To measure the R-2I RNA binding activity, the fractions were dialyzed overnight against 1X binding buffer and then analyzed in an RNA EMSA experiment. As shown in Fig. 5.10B, the amount of R-2I/protein complex formed closely correlates with the elution profile for the 36-kDa protein. The ratio of binding activity to the amount of 36-kDa protein quantified by silver staining was nearly constant across the elution profile (Fig. 5.10C) suggesting that this protein is the pH-RE binding protein. To further support this conclusion, the affinity purification was repeated using a shallower gradient of the

Fig. 5.8. Protein profile during gradient elution.

Panel A. After an extensive wash with 1X binding buffer, the buffer concentration was gradually increased to 20X. The protein concentration in the eluant was monitored as absorbance at 260 nm.

Panel B. After an extensive wash with 1X binding buffer, a step-wise gradient was applied. The protein concentration in the eluant was monitored as absorbance at 260 nm.

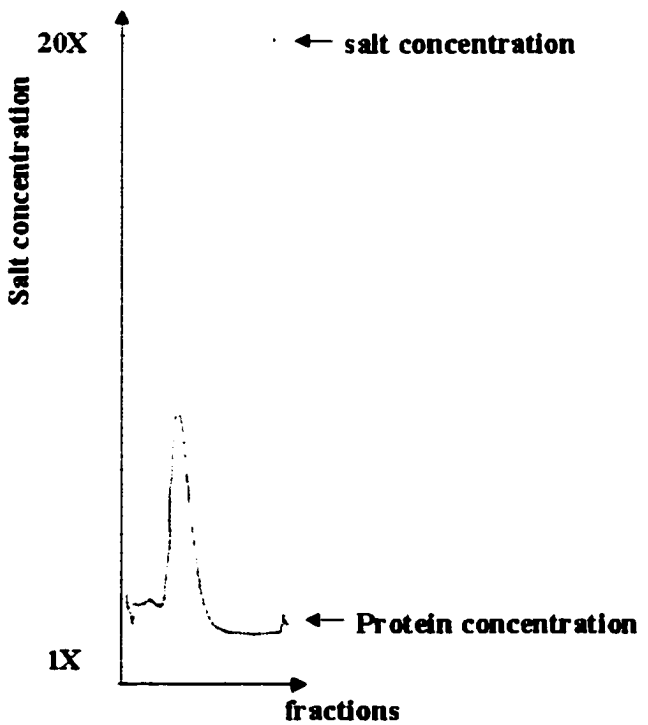

Fig. 5.8A

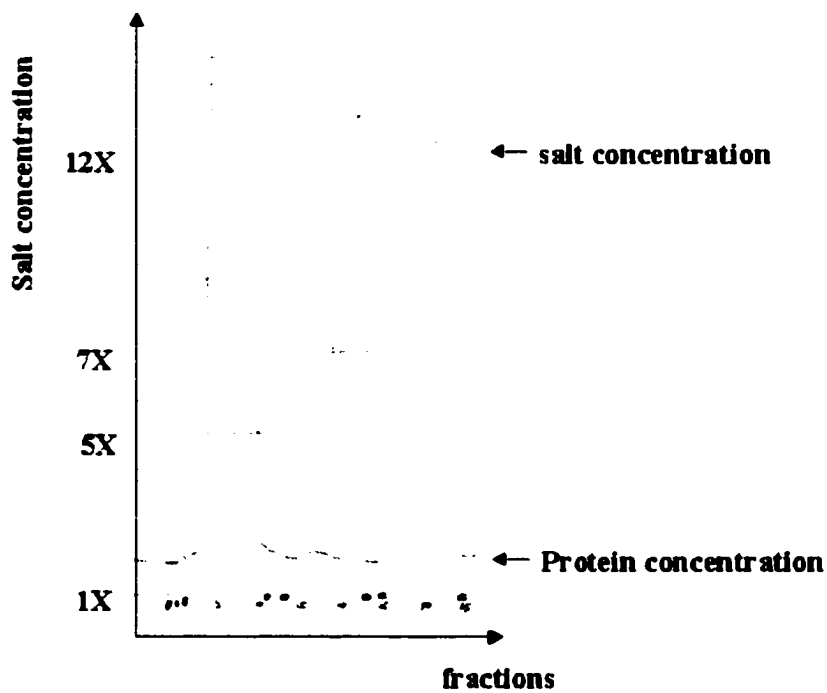

Fig. 5.8B

Fig. 5.9. Salt gradient used to elute the pHRE binding protein from the avidin agarose column.

A crude rat kidney extract was incubated with the synthesized ligand and then applied to an avidin-agarose column. The column was washed with the indicated gradient profile. The eluant from the steep increase in salt concentration was collected in ten 0.5-ml fractions.

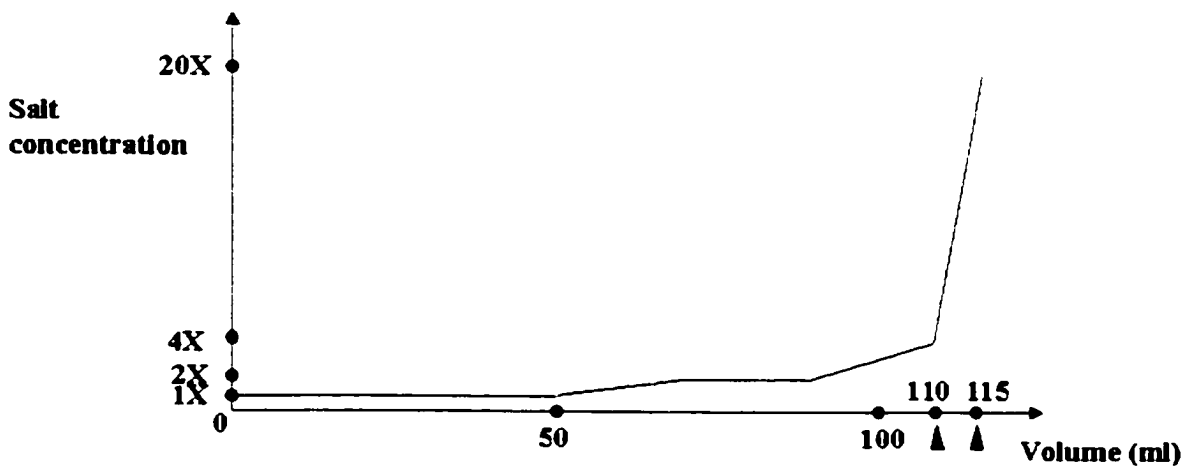

Fig. 5.9

4X to 20X binding buffer in order to separate the proteins into 28 fractions. Analysis by SDS-PAGE and silver staining (data not shown) indicated that fraction 13 contained only the 43-kDa protein, whereas fraction 20 contained only the 36-kDa protein. After dialysis, the two fractions were tested for R-2I RNA binding activity (Fig. 5.11). Again, only the fraction containing the 36-kDa protein formed a RNA/protein complex. The fraction containing the 43-kDa protein neither bound the R-2I RNA nor affected the level or mobility of the complex formed with the 36-kDa protein. Thus, the purified 43-kDa protein does not form a specific complex with the R-2I RNA.

The purified, 36 kDa protein was applied to NEpHGE analysis (Fig. 5.12). There appear to be multiple forms of this protein with slightly different pIs. This may imply multiple phosphorylations on this protein.

5.3.3. Competition experiment for purified protein.

Competition experiments were performed to determine the specificity of the binding interaction between the purified pH-RE binding protein and the R-2I RNA (Fig. 5.13A). As a control, the same binding experiment was performed using a cytosolic extract of rat renal cortex (Fig. 5.13B). The complexes produced with both protein samples exhibited identical electrophoretic mobilities. A 100-fold excess of various unlabeled RNA was added to compare specificity. The mut1, mut2, and mut3 competitors were R-2I RNA in which the first, second, and both of the AU-rich regions were mutated, respectively. The $(AUUU)_5A$ RNA contains five tandem repeats of an AUUUA sequence. This sequence binds a variety of AUUUA binding proteins (Chen, 1995). The pBS RNA was transcribed from the multicloning site of pBlueScript II SK(+) and was included as a non-specific competitor. Finally, the R-2H RNA is a 76-nucleotide

Fig. 5.10. Analyses of samples collected from the avidin agarose column.

Panel A. Aliquots of fractions 4 - 9 were dialyzed overnight against 1X binding buffer and then separated by 10% SDS-PAGE and silver stained.

Panel B. Aliquots of the same fractions were analyzed for binding activity using an RNA gel-shift assay containing 25 fmol of ^{32}P-labeled R-2I RNA.

Panel C. Specific binding activity was estimated as the ratio of the digitized intensities of the protein/RNA complex observed in panel B divided by that of the 36-kDa protein from Panel A.

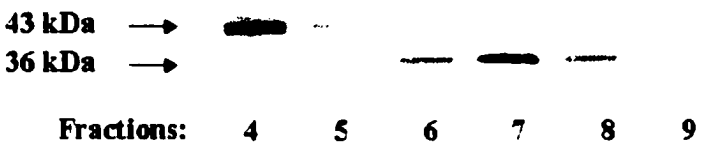

Fig. 5.10A

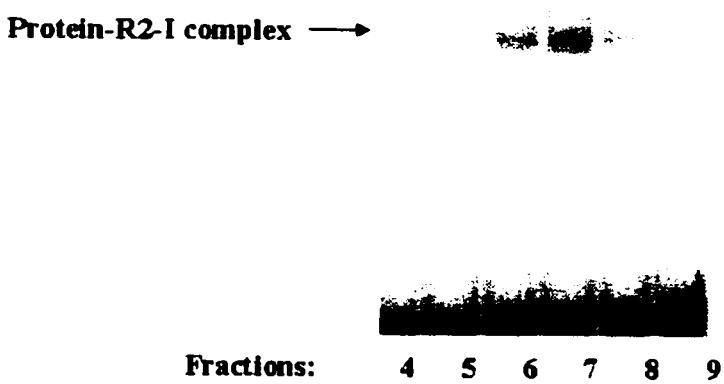

Fig. 5.10B

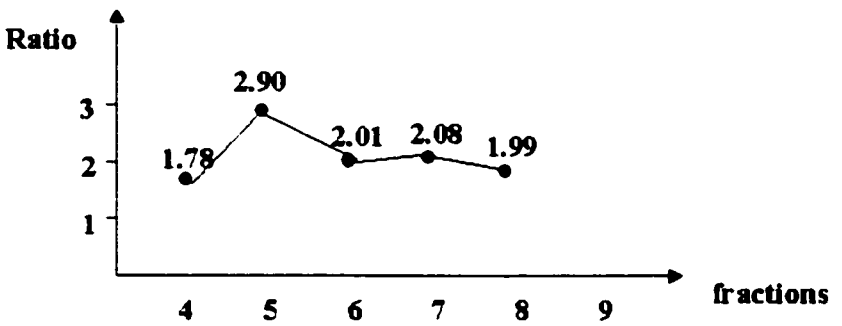

Fig. 5.10C

sequence that includes all of R-2I plus flanking sequences from the GA mRNA. Formation of the protein/R-2I complex with either the purified protein or the crude extract was almost completely inhibited by the R-2H RNA. In addition, both complexes were slightly competed by the $(AUUU)_5A$ and mut2 RNAs, but not by any of the other RNAs. Thus, the purified pH-RE binding protein exhibits a specificity identical to that observed with the crude extract.

5.3.4. Purification, tryptic digestion and microsequencing.

The purified and concentrated pH-RE binding protein was subjected to SDS-PAGE and stained with Coomassie Blue. The 36-kDa protein band was cut from the gel, digested with trypsin, and sequenced by mass spectroscopy. A total of 13 peptides were identified. The peptides were classified into two groups. Class I peptides (Fig. 5.14) include eight sequences that are identical to tryptic peptides derived from the 36-kDa mouse ζ-crystallin /NADPH:quinone reductase protein. Three other Class I peptides differ from tryptic peptides of mouse ζ-crystallin by a single amino acid substitution and may represent sequences from the rat homologue. The two Class II peptides (Fig. 5.15) correspond to trypic peptides contained in the 43-kDa mouse RNA binding protein, TIAR.

5.3.5. Western analysis of purified protein.

The identities of the two proteins contained in the purified preparation of the pH-RE binding protein were confirmed by western blot analysis. Antisera produced against the full-length ζ-crystallin/NADPH:quinone reductase purified from guinea pig lens

Fig. 5.11. Comparison of the binding activities observed with fractions that contained either the 36-kDa or the 43-kDa proteins.

Samples containing approximately 10 ng of protein from each fraction were incubated with 25 fmol of ^{32}P-labeled R-2I RNA and then separated on a native polyacrylamide gel.

36 kDa protein:	--	--	+	+
43 kDa protein:	--	+	--	+

1 2 3 4

Fig. 5.11

Fig. 5.12. 2-Dimentional electrophoresis of the pHRE-BP.

The purified pHRE-BP was subjected to analyses using non-equilibrium pH gradient electrophoresis and SDS-PAGE. The 36-kDa protein was fractionated into four separate bands that had apparent pIs between 5.7 and 6.4.

Fig. 5.12

Fig. 5.13. Comparison of the binding specificity of the pHRE binding activity of a crude extract and the purified protein.

Samples containing 25 fmol of ^{32}P-labeled R-2I RNA were incubated either in the absence (lane 1) or presence (lanes 2-8) of either 3 μg of a cytosolic extract of rat kidney cortex (Panel A) or 10 ng of purified pHRE binding protein (Panel B). Samples in lanes 3-8 also contained a 100-fold excess of the indicated competitor.

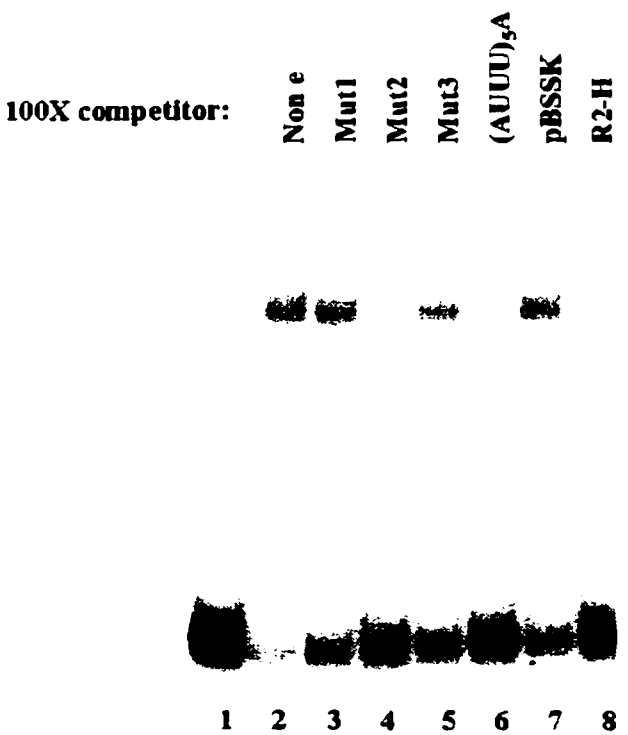

Fig. 5.13A

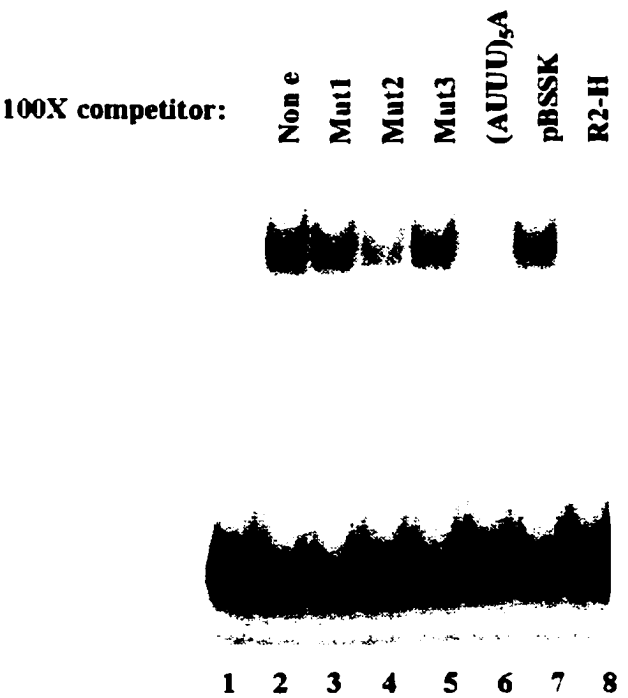

Fig. 5.13B

reacted with only the single 36-kDa protein when tested versus a crude cytosolic extract of rat renal cortex (Fig. 5.16). The same reaction was observed with fraction 7 from purification (see Fig. 5.10A). When used versus a purified sample containing both the 43- and 36-kDa proteins (Fig. 5.17), the anti-ζ-crystallin antibody again bound only to the 36-kDa protein. Similarly, a monoclonal antibody, that is specific for TIAR, bound to only the 43-kDa protein. Thus, a slight contamination of the isolated 36-kDa protein band with the larger protein accounts for the two Class II peptides that were identified by microsequencing.

5.3.6. Immunoblocking experiment.

Immunoblocking assays were performed to confirm that ζ-crystallin/NADPH:quinone reductase is a pH-RE binding protein. Preincubation of a cytosolic extract of rat renal cortex with increasing amounts of anti-ζ-crystallin antiserum completely blocked the formation of the specific R-2I RNA/protein complex (Fig. 5.18A). The same inhibition pattern was observed when the gel-shifts were performed with the purified pH-RE binding protein (See Fig. 5.18B). The observed inhibition was specific since anti-glutaminase antiserum had no effect on the complex formation (in lane 6). The affinity ligand used to purify the pH-RE binding protein was slightly longer than the R-2I RNA probe. Thus, labeled R-2H RNA, which contains all of the ribonucleotides present in the RNA affinity ligand, was synthesized and used as a probe for gel-shift analysis (Fig. 5.18B). Because of the larger size of this probe, the resulting complex was digested with RNase T1 before electrophoresis. Again, the resulting complex is completely blocked by preincubation with anti-ζ-crystallin antiserum but is not affected

Fig. 5.14. Class I peptides identified by mass spectroscopy.

Eight of the identified peptides (solid underline) were a perfect match to sequences found in mouse ζ-crystallin/NADPH quinone reductase. Three other peptides (dashed underline) differed from sequences found in mouse ζ-crystallin/NADPH quinone reductase by only the single amino acid shown by the arrow.

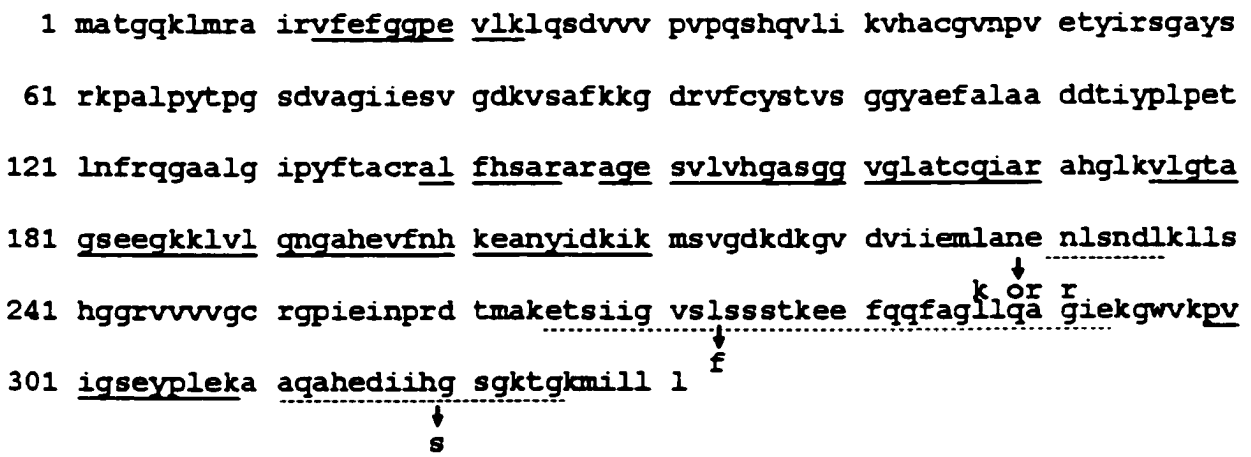

Fig. 5.14

Fig. 5.15. Class II peptides identified by mass spectroscopy.

Two of the identified peptides (solid underline) were a perfect match to sequences found in the mouse TIAR protein.

```
  1 mmeddgqprt lyvgnlsrdv tevlilqlfs qigpcksckm iteqpdsrrv nssvgfsvlq
 61 htsndpycfv efyehrdaaa alaamngrki lgkevkvnwa ttpssqkkdt snhfhvfvgd
121 lspeittedi ksafapfgki sdarvvkdma tgkskgygfv sfynkldaen aivhmggqwl
181 ggrqirtnwa trkppapkst qetntkqlrf edvvnqsspk nctvycggia sgltdqlmrq
241 tfspfgqime irvfpekgys fvrfsthesa ahaivsvngt tieghvvkcy wgkespdmtk
301 nfqqvdysqw gqwsqvygnp qqygqymang wqvppygvyg qpwnqqgfgv dqspsaawmg
361 gfgaqppqgq apppvipppn qagygmasfp tq
```

Fig. 5.15

Fig. 5.16. Western blot analysis of a crude kidney extract and the purified protein using anti-ζ-crystallin antibodies.

Samples containing 0.5 µl of a crude kidney extract (lane 1) or 10 µl of the purified kidney protein (lane 2) were fractionated on a 10% SDS-PAGE. For western blot analysis, anti-ζ-crystallin serum from rabbit was used as primary antibody. HRP-conjugated goat anti-rabbit IgG antibody was used as secondary antibody. Results were visualized using ECL-plus kit and the STORM instrument.

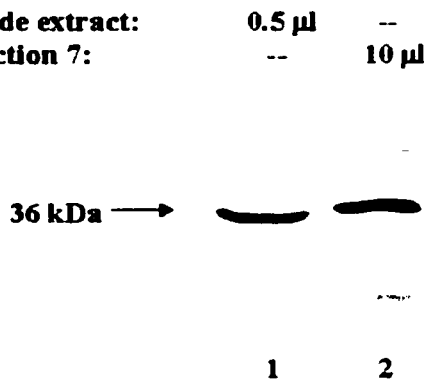

Fig. 5.16

Fig. 5.17. Western blot analysis of the purified binding protein using anti-ζ-crystallin and anti-TIAR antibodies.

Samples containing 10 µl of the purified binding protein were fractionated on a 10% SDS-PAGE. Anti-ζ-crystallin rabbit serum (lane 1) or purified anti-TIAR antibody (lane 2) was used as the primary antibody. HRP-conjugated goat anti-rabbit IgG antibody was used as the secondary antibody. Results were visualized using ECL-plus kit and the STORM instrument.

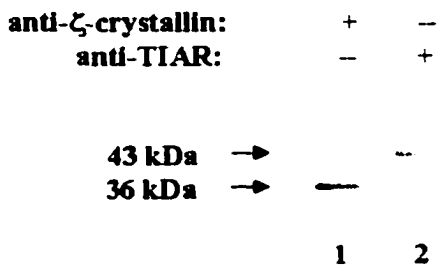

Fig. 5.17

by pretreatment with antibody specific for TIAR. Thus, ζ-crystallin/NADPH: quinone reductase binds with high affinity and specificity to the pH-RE.

5.4. Expression of recombinant ζ-crystallin

5.4.1. Induction of ζ-crystallin expression in *E. coli*

ζ-crystallin was cloned into pET-3a and pET-15b vectors and expressed in *E. coli* DE3 cells. At different time intervals after IPTG induction (0, 2, 4h), 40 ml of DE3 cells were used to prepare a cytosolic extract. As a control, DE3 cells were transformed with the parent pET-3a vector and an extract was prepared without induction.

As illustrated by a 10% SDS-PAGE, ζ-crystallin encoded by pET-3a vector did not show a significant induction (Fig 19A). This was true even when the induction time was increased to 7h. However, with the pET-15b-zeta vector significant induction of ζ-crystallin expression was evident (Fig 19B). The expressed protein also contains an N-terminal His tag and the thrombin cleavage site. Therefore it is slightly larger than a full-length ζ-crystallin.

The same set of samples from pET-15b-zeta induction was used in a western experiment, which confirmed that expression of ζ-crystallin had occurred (Fig. 20A). If pET-3a-zeta was compared against pET-15b-zeta (Fig. 20B) in a similar experiment, very low, if any, induction was observed.

Fig. 5.18. Immunoblocking analysis of the pH-RE binding protein.

Panel A. Samples containing either zero (lane 1) or 3 μg (lanes 2-6) of a crude extract were preincubated with increasing amounts (0.25 μg, 0.5 μg, or 1 μg) of ζ-crystallin antiserum or 1 μg of glutaminase antiserum. Then 25 fmol of ^{32}P-labeled R-2I RNA were added and the samples were separated on a native polyacrylamide gel.

Panel B. Samples containing either zero (lane 1) or 5 ng of purified protein (lanes 2-4) were preincubated with either 1 μg of ζ-crystallin antiserum or 4 μg of TIAR monoclonal antibody. Then 10 fmol of ^{32}P-labeled R-2H RNA were added and the samples were digested with RNase T1 and separated on a native polyacrylamide gel.

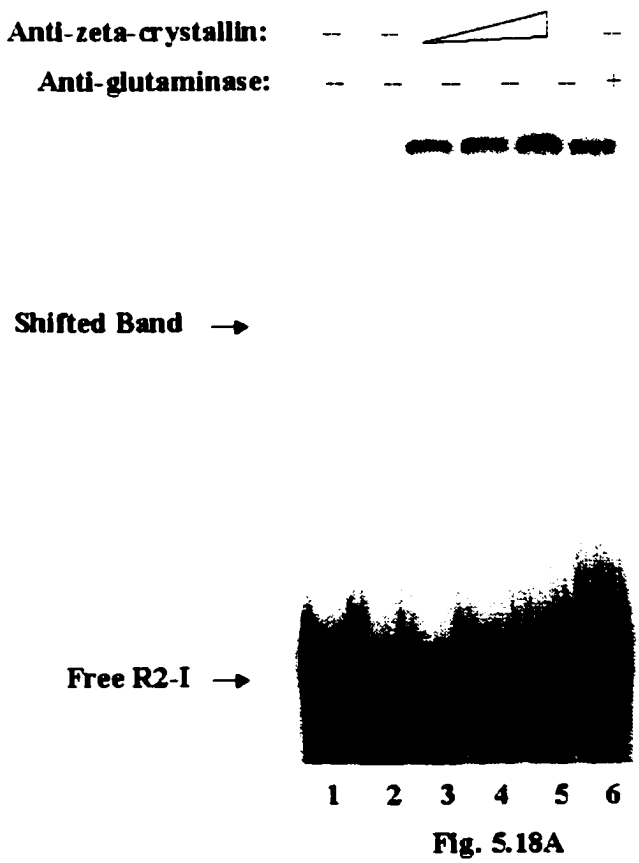

Fig. 5.18A

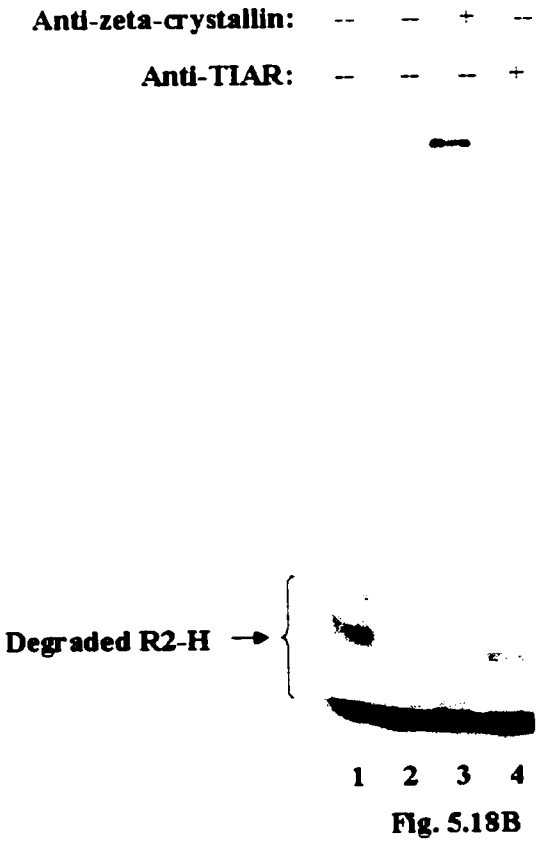

Fig. 5.18B

Fig. 5.19. Expression of ζ-crystallin in E. coli.

Panel A. The DE3 strain of *E. coli* was transformed with pET-3a-zeta plasmid. The culture was induced with IPTG. Samples containing 40 ml of *E. coli* cells were obtained at different intervals after induction (0, 0.5, 1, 2, 3, and 5h) and cytosolic extract were prepared. Aliquots of the different extracts were separated by SDS-PAGE and the proteins were visualized by Coomassie Blue staining.

Panel B. The DE3 strain of *E. coli* was transformed with pET-15b-zeta plasmid. The culture was induced with IPTG. Samples containing 40 ml of *E. coli* cells were obtained at different intervals after induction (0, 0.5, 1, 2, 3, and 5h) and cytosolic extract were prepared. Aliquots of the different extracts were separated by SDS-PAGE and the proteins were visualized by Coomassie Blue staining.

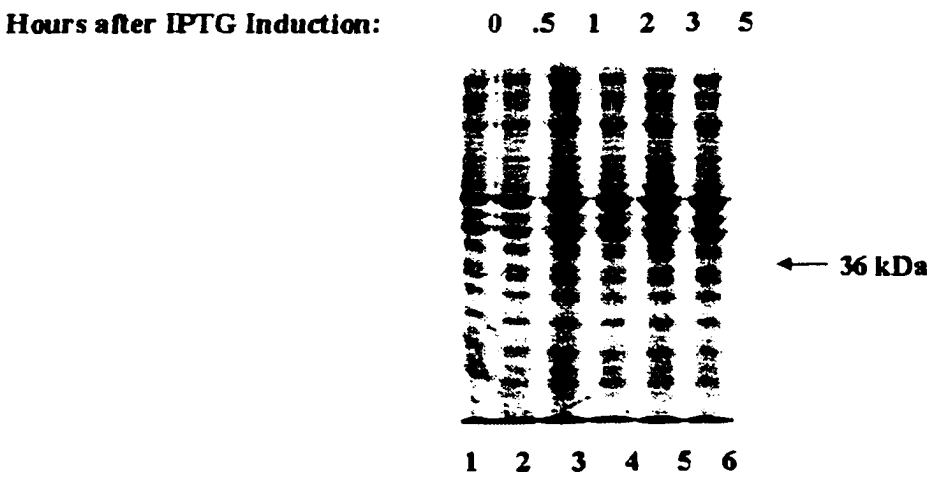

Fig. 5.19A

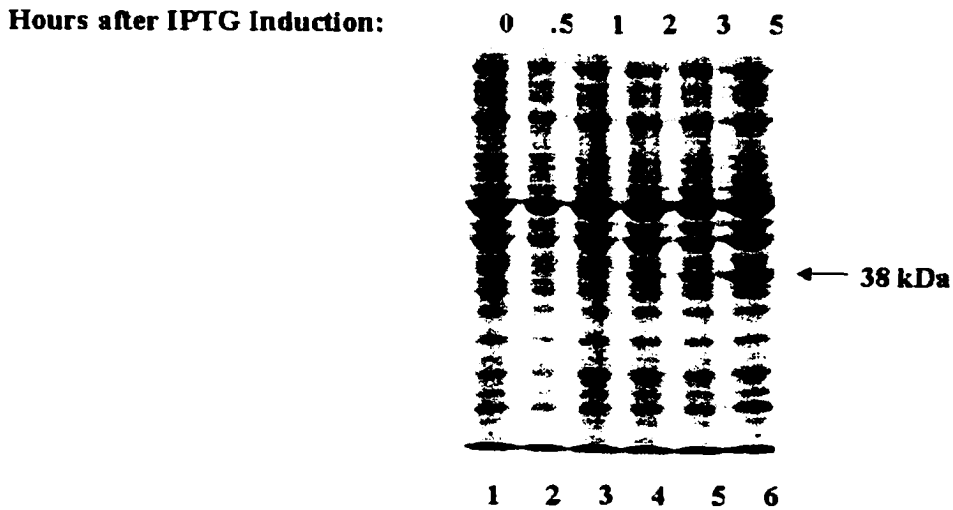

Fig. 5.19B

Fig. 5.20. Western blot analysis of ζ-crystallin expression in E. coli.

Panel A. The same gel shown in Fig. 5.18B was used for western blot analysis. Anti-ζ-crystallin serum from rabbit was used as primary antibody. HRP-conjugated goat anti-rabbit IgG antibody was used as secondary antibody. Results were visualized using the ECL-plus kit and the STORM instrument.

Panel B. In another preparation, the DE3 strain of *E. coli* was transformed with pET-3a-zeta (lanes 2, 3, and 4) or pET-15b-zeta (lanes 5, 6, and 7). DE3 cells transformed with pET-3a (lane 1) was also included as a control. The induction times were shown in the figure. Anti-ζ-crystallin serum from rabbit was used as primary antibody. HRP-conjugated goat anti-rabbit IgG antibody was used as secondary antibody. Results were visualized using the ECL-plus kit and the STORM instrument.

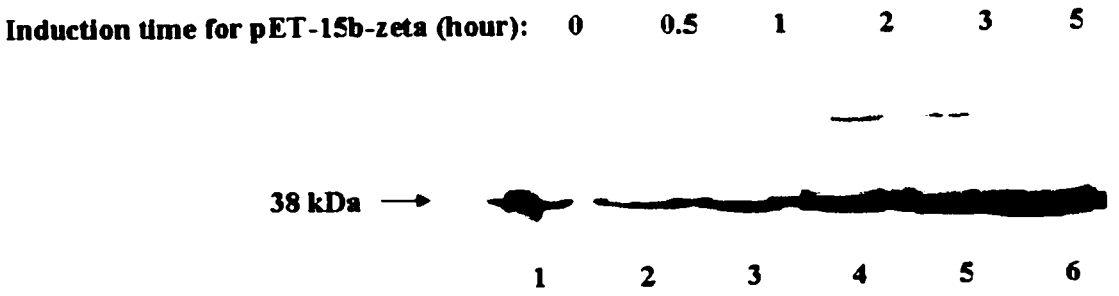

Fig. 5.20A

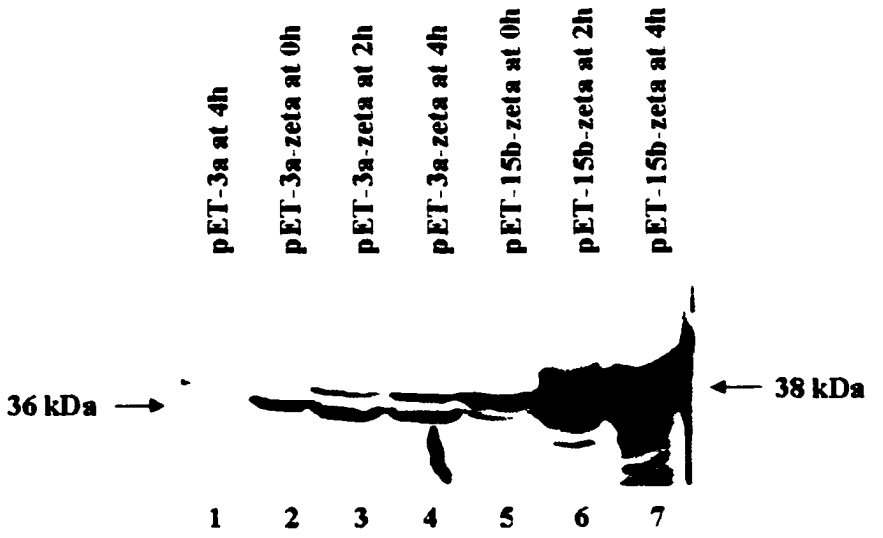

Fig. 5.20B

5.4.2 Induction of ζ-crystallin expression in LLC-PK_1-F^+ cells

ζ-crystallin was also cloned into pcDNA3.1 vector to transfect LLC-PK_1-F^- cells. Cells from a 10 cm plate were collected to prepare a cytosolic extract. Samples containing 20 μg of total protein from expressing cells (E1 and E2, shown in lane 2 and 3) or from control cells (C1 and C2, shown in lane 4 and 5) were used for western blot analysis. Over-expression was significant in both E1 and E2 plates (Fig. 21).

There were some smaller peptides that cross-reacted with ζ-crystallin antibody. A peptide with a similar molecular weight was observed in samples of purified protein. Because of their absence in control plates, these peptides were speculated to be fragments of ζ-crystallin that are generated by proteolysis.

5.4.3. RNA EMSA with recombinant ζ-crystallin from *E. coli.*

ζ-crystallin expressed from both the pET-3a and pET-15b vectors were tested. Extracts were made after different times of induction, and the same volume of samples were used for both SDS-PAGE and RNA EMSA. The total protein per sample was not normalized in this experiment. However, the actual amount of protein per sample probably increased with the time of induction and number of cell divisions.

Surprisingly, the control extracts contained a protein that binds to the R-2I RNA with a similar mobility as pHRE-BP (Fig. 22A, and C). Furthermore, extracts that contain the recombinant ζ-crystallin did not show a proportional increase in binding activity

Fig. 5.21. Western blot analysis of ζ-crystallin expression in LLC-PK$_1$-F$^+$ cells. LLC-PK$_1$-F$^-$ cells were transfected with pcDNA3.1-zeta plasmid (lanes 4 and 5). As a control, cells transfected with the pcDNA3.1 plasmid (lanes 2 and 3) and purified ζ-crystallin (lane 1) were included as controls. Anti-ζ-crystallin serum from rabbit was used as primary antibody. HRP-conjugated goat anti-rabbit IgG antibody was used as secondary antibody. The results were visualized using the ECL-plus kit and the STORM instrument.

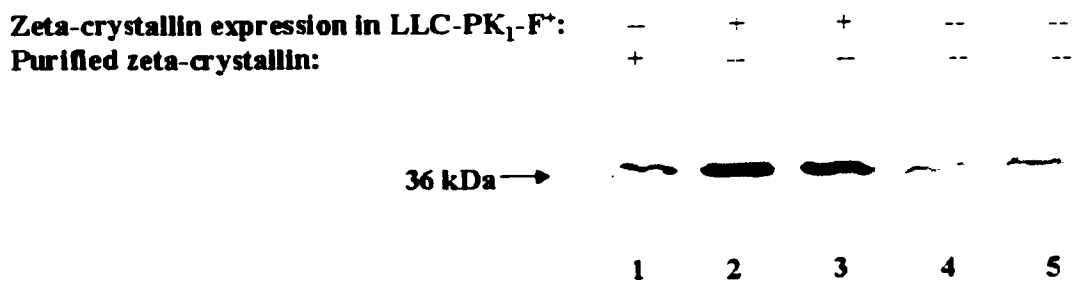

Fig. 5.21

(Fig. 22B and D). The slight change in intensity at different intervals after induction was attributable to experimental errors and non-standardization of added protein. Considering the significant induction as evidenced by the SDS-PAGE and western blot analysis, the observed binding must be due to an endogenous *E. coli* protein, and not the bacterially expressed ζ-crystallin. The identity of this protein is unknown.

A crude extract from *E. coli* expressing pET-15b-zeta was applied to a Ni column, and the His tag on its N-terminus was cleaved (Fig. 23). The resulting recombinant ζ-crystallin failed to show affinity toward R2-I.

5.4.4. RNA EMSA with recombinant ζ-crystallin from LLC-PK$_1$-F$^+$.

RNA EMSA experiment with extract from LLC-PK$_1$-F$^+$ cells revealed the following (Fig. 24):

1. Degradation of the R-2I RNA during incubation was much greater than with the rat kidney extract. The reason for this was not clear, but is consistent with observations made previously (Laterza et al., 2000). This degradation needs to be prevented before binding with LLC-PK$_1$-F$^+$ cell extracts can be accurately quantified.
2. E1 and E2 (two plates that were transfected with pcDNA3.1-zeta) provided increased protection of the R-2I RNA.
3. The binding observed with E1 and E2 was apparently greater than that observed with C1 and C2 (two control plates). However, the mobility of the resulting complex was much slower than that observed with the purified ζ-crystallin. This

binding is potentially from the expressed ζ-crystallin, possibly in complex with other unknown proteins. Immunoblocking of this complex was not very obvious when ζ-crystallin antiserum was applied. A decisive conclusion can be drawn only after the degradation problem is resolved.

Fig. 5.22. Characterization of the pHRE binding activity of bacterially expressed ζ-crystallin.

Samples containing 40 ml of *E. coli* DE3 cells that were transformed with pET-3a (Panel A), pET-3a-zeta (Panel B), pET-15b (Panel C), or pET-15b-zeta (Panel D) were collected at different intervals after IPTG induction (0, 0.5, 1, 2, 3, 5, and 7 hour) and were used to prepare extracts. As controls, 3 μg of a crude extract from rat kidney (lane 2) and 1 – 4 μl of purified ζ-crystallin (lane 3) were also included. RNA EMSA was performed using 25 fmol of ^{32}P-UTP labeled R-2I (RNA). The samples were resolved by native PAGE and visualized on a STORM instrument.

3 µg crude extract:	–	+	–	--	--	–	--	--	--	--
1 µl purified zeta-crystallin:	–	--	+	--	--	--	--	--	--	--
6 µl E. coli extract (transformed with pET-3a) after induction (hour):	–	–	–	**0**	**.5**	**1**	**2**	**3**	**5**	**7**

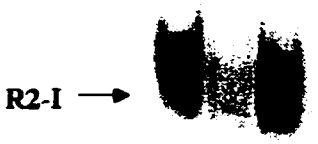

1 2 3 4 5 6 7 8 9 10

Fig. 5.22A

3 μg crude extract:	–	+	–	–	–	–	–	–	–
6 μl E. coli extract (transformed with pET-3a-zeta) after induction (hour):	–	–	**0**	**.5**	**1**	**2**	**3**	**5**	**7**

1 2 3 4 5 6 7 8 9

Fig. 5.22B

3 µg crude extract:	–	+	–	–	–	–	–	–	–	–
4 µl purified zeta-crystallin:	–	–	+	–	–	–	–	–	–	–
6 µl E. coli extract (transformed with pET-15b) after induction (hour):	–	–	–	**0**	**.5**	**1**	**2**	**3**	**5**	**7**

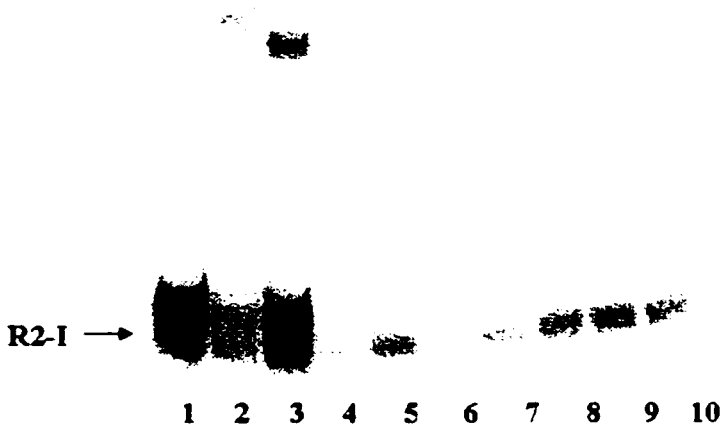

Fig. 5.22C

3 µg crude extract:	--	+	--	--	--	--	--	--	--	--
1 µl purified zeta-crystallin:	--	--	+	--	--	--	--	--	--	--
6 µl E. coli extract (transformed with pET-15b-zeta) after induction (hour):	--	--	--	**0**	**.5**	**1**	**2**	**3**	**5**	**7**

Fig. 5.22D

Fig. 5.23. Purification of bacterially expressed ζ-crystallin using pET-15b-zeta plasmid.

Samples containing a crude extract of DE3 cells that expressed the pET-15b-zeta plasmid (lane 1), the recombinant ζ-crystallin that was purified on a Ni column and partially digested with thrombin (lane 2), and the purified protein after complete thrombin treatment (lane 3) were analyzed on a 10% SDS-PAGE.

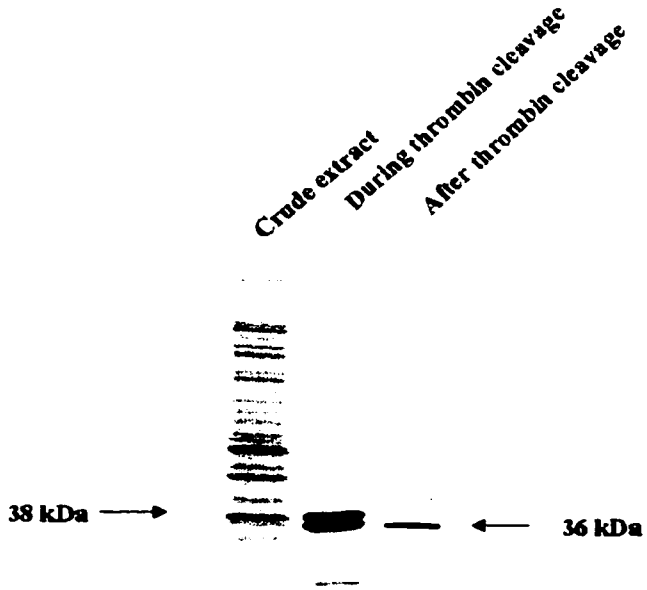

Fig. 5.23

Fig. 5.24. Characterization of the pHRE binding activity of ζ-crystallin expressed in LLC-PK$_1$-F$^+$ cells.

10 cm plates of LLC-PK$_1$-F$^+$ cells that were transfected with pcDNA3.1-zeta or the pcDNA3.1 control plasmid were used to make cytosolic extracts. RNA EMSA was performed using 25 fmol of [α-^{32}P]-UTP labeled R-2I RNA and 10 μg of extracts from control (C) cells (lanes 4, 5 & 8) or cells that express (E) ζ-crystallin (lanes 6, 7 & 9) were used. As controls, 3 μg of crude extract from rat kidney cortex (lanes 2 & 3) were included. Where indicated, 1 μg of ζ-crystallin antiserum was preincubated with extract (lanes 8 & 9). The samples were resolved by native PAGE and visualized on a STORM instrument.

Crude extract:	--	+	+	--	--	--	--	--	--
Anti-zeta-crystallin:	--	--	+	--	--	--	--	+	+
F+ cell extract (expressing zeta-crystallin):	--	--	--	--	--	+	+	--	+
F+ cell extract (control):	--	--	--	+	+	--	--	+	--

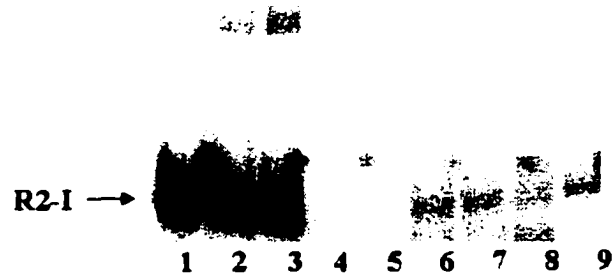

Fig. 5.24

6. Discussion and future directions

6. DISCUSSION AND FUTURE DIRECTIONS

Many labile mRNAs that encode cytokine, lymphokine and proto-oncogene products, contain AU-rich elements (AUREs) in their 3'-UTR. Regulation of the expression of these proteins is accomplished, in part, through changes in protein binding to these elements in response to various extracellular stimuli. Thus, specific trans-acting proteins are responsible for regulating mRNA stability through interactions with the AUREs. In this work, the binding protein that interacts with the 3'-UTR of mitochondrial glutaminase mRNA from rat kidney was identified as ζ-crystallin/NADPH:quinone reductase.

6.1. Evolution of the purification scheme.

Previous studies have established that the rat renal GA mRNA contains a direct repeat of an eight-nucleotide AU-sequence that functions to stabilize the GA mRNA during metabolic acidosis. Cytosolic extracts of rat kidney cortex and of LLC-PK_1-F^+ cells contain a protein that binds to the identified pHRE with high affinity. The binding activities in the two extracts are increased following onset of acute acidosis or treatment with acidic medium, respectively. Thus, the protein that binds to the pH-RE apparently functions to stabilize the GA mRNA (Laterza et al., 1997, 2000). Using the general approach developed by Rouault et al. (1989), we designed an approach to purify the binding protein using the pH-RE as the affinity ligand. A preliminary calculation (shown below) indicated that, if 90% efficiency was achieved in purification, 2 ml of cytosolic extract from rat kidney cortex would generate enough proteins for sequencing. This

amount could be obtained from 2 to 3 pairs of rat kidneys. The relatively high abundance of pHRE-BP made the purification much easier.

$500 * 10^{-12}$ mol * 48000 g/mol / 90% / 0.05% / 25 mg/ml = 2 ml

In the equation above, 500 pmol is the desired amount of pHRE-BP for sequencing. 48000 g/mol is the molecular weight of pHRE-BP (originally estimated from a UV-crosslinking experiment), 90% is the assumed purification efficiency, 0.05% is the estimated abundance of pHRE-BP in cytosolic proteins, and 25 mg/ml is the total protein concentration of a typical rat kidney cytosolic extract.

Another limiting reagent was the ligand. In a 10-µl *in vitro* transcription reaction, 2.3 µg of R-2I were obtained. This is equivalent to 240 pmols of RNA (shown in the following calculation). To achieve high efficiency binding, the amount of ligand should exceed that of the binding protein by several fold. Therefore, multiple *in vitro* transcription reactions would have been needed to obtain sufficient ligand. Using R-2H, instead of R-2I would require even more transcriptions.

$2.3 * 10^{-6}$ g / (330 * 29 g/mol) = 240 pmol

In the above equation, 29 is the length of R-2I. 330 is the average molecular weight of a nucleotide.

The other reagents can be purchased and thus were not a limitation.

R-2I contained less flanking sequences than R-2H. Thus, R-2I was used initially to avoid non-specific binding. However, as shown in Table 5.1, biotinylated R-2I failed to bind to avidin agarose. Since this was true whether or not extract was added, we proposed that R-2I adopts a three-dimensional structure such that the 3'-end (where biotinylation occurred) was buried and not accessible.

This problem was solved by using R-2H RNA, which contains more biotinylation sites. The adequate binding of biotinylated R2-H RNA was confirmed in the experiment described in Table 5.1.

The small-scale purification using biotinylated R-2H RNA provided initial success in obtaining some purified pHRE-BP. However, the loss during the washing steps was too high to achieve the desired 90% recovery. Thus, modifications to the purification scheme were necessary.

The first change was to design a new ligand. During *in vitro* transcription, the RNA polymerase chooses either CTP or biotinylated CTP from the nucleotide pool. The resulting product was therefore a heterogeneous mixture with regard to biotinylation sites. This was potentially a problem when the ligand was applied to the avidin agarose column. For example, some of the ligand may no longer form a complex with the binding protein due to structural constraints imposed by biotin-avidin interactions on both ends of the ligand.

In previous studies, a synthesized RNA ligand was used to purify a β-actin mRNA zipcode-binding protein (Ross A. F., 1997). This approach was tested and preliminary experiments confirmed the many advantages of using a synthesized ligand (section 5.2).

Another change was made based upon advice from Dr. Craig Martens to improve control during the washing and elution steps. Initially manual washing was used in which a set of buffers with increasing salt concentration was applied sequentially to the column to achieve a stepwise gradient. This protocol involved considerable work to fine tune the gradient. Furthermore, controlling the flow rate and avoiding disturbance when adding

buffer presented a challenge. By using an FPLC system, many of the problems were solved and a highly reproducible gradient was generated.

It was also necessary to dialyze the crude extract overnight against 1X binding buffer before applying it to the column. This did not affect pHRE-binding activity to a significant extent, but did improve the fold purification. In purifications where pre-dialysis was omitted (data not shown), the eluants containing the purified protein also contained many other proteins as evident by SDS-PAGE analysis. These proteins may represent ones that interact with the pHRE-BP without binding specifically to the pHRE.

6.2 Identification of the pHRE-BP.

Identification of the pHRE-BP included two steps: 1. Demonstration that protein purified to > 90% homogeneity exhibits the same binding properties as observed with a crude extract. 2. Sequence analysis of the purified protein. This two-step verification was done in the following experiments.

In an RNA-EMSA, the purified protein formed a complex with the R-2I RNA that retained the same electrophoretic mobility and specificity as observed with the crude cytosolic extract. In both cases, the observed binding was strongly competed by an oligonucleotide (R-2H) that contained both AU-elements. When characterized as independent binding sites, the initial eight-nucleotide element of the direct repeat was shown to have greater affinity for the pH-RE binding protein. These data are consistent with the observation that the mut2 oligonucleotide, which retains the initial eight-base element, functions as a weak competitor. The $(AUUU)_5A$ oligonucleotide was previously shown to be a weak competitor. None of the other tested oligonucleotides were able to compete the specific binding observed with either the crude extract or the

purified pH-RE binding protein. Thus, the binding activity observed with the purified protein and the crude extract from rat kidney cortex are likely to be properties of the same binding protein.

The preparation of purified pH-RE binding protein contained two proteins that were identified by MS/MS sequencing and Western blot analysis. One of the proteins is the T-cell restricted intracellular antigen-related protein (TIAR), a well-known RNA-binding protein that contains three RNA recognition motifs (Dember et al., 1996). TIAR may participate in Fas-mediated apoptotic cell death (Taupin et al., 1995 and Kawakami et al., 1992). It also binds to the AU-rich element that mediates the translational regulation of tumor necrosis factor α mRNA (Gueydan et al., 1999). An *in vitro* analysis of its binding preference revealed that TIAR also has an affinity for RNAs that contain short stretches of uridylate residues. This broad specificity may account for the purification of TIAR by the AU-rich pH-RE affinity ligand. However, the purified TIAR failed to gel shift either the R-2I or the longer R-2H RNA. In addition, specific antibodies to TIAR did not block formation of specific complexes that are formed by incubating either RNA with a cytosolic extract of rat kidney cortex. Thus, it is unlikely that TIAR functions as a pH-RE binding protein. However, it remains possible that the purified TIAR is irreversibly denatured by the high concentration of salt contained in the elution buffer. Thus, the potential role of TIAR in the pH-responsive stabilization of GA mRNA should be tested using the recombinantly expressed protein.

The second protein identified in the purified preparation of the pH-RE binding protein was ζ-crystallin/NADPH:quinone reductase. ζ-crystallin constitutes 10 percent of the total protein present in the lens of hystricomorph rodents and camelids. In these

species, the ζ-crystallin gene contains an alternative promoter that accounts for its lens-specific over-expression (Gonzalez et al., 1995). Similar to other lens crystallins with a limited phylogenetic distribution, ζ-crystallin also has a catalytic activity and is expressed at enzymatic levels in various tissues of different species. ζ-crystallin possesses a novel NADPH-dependent quinone reductase activity that reduces various quinones through the sequential transfer of single electrons.

When elution was performed with high-salt buffer, two proteins were always present, one with a mass of 43 kDa, the other 36 kDa. However, after dialysis, only the smaller protein bound to the pHRE. The resulting complex exhibited the same mobility and specificity as the complex formed using a crude extract. Therefore, only the band corresponding to the smaller protein was isolated for sequencing. The following evidence supports that ζ-crystallin/NADPH:quinone reductase is the pHRE-BP. 1. ζ-crystallin has a molecular weight of 36 kDa. This is consistent with the size of the protein from the excised band. 2. Many peptides from the sample are identical or homologous to the mouse ζ-crystallin sequence. Taken together, these peptides covered a segment of ζ-crystallin that extended from the N-terminal to the C-terminal. 3. Antiserum against ζ-crystallin cross-reacts with the 36-kDa protein by immunoblocking. 4. Antiserum against ζ-crystallin blocks formation of the complex that is generated using R-2I RNA and a crude extract.

The larger protein recovered from the purification protocol is likely to be TIAR. When the sample for sequencing was prepared, a small percentage of the TIAR apparently migrated with a higher mobility into the 36-kDa region. This may explain why only two peptides from TIAR were identified. This conclusion was confirmed by a

western blotting which demonstrated that the 43-kDa protein cross-reacted with the anti-TIAR IgG antibody.

ζ-Crystallin/NADPH:quinone reductase was not previously known to function as an RNA-binding protein. However, the ability of bovine ζ-crystallin to bind to different forms of DNAs had been quantified through an ELISA assay. It preferentially binds to double-stranded Z-DNA and to single-stranded DNA but has a 5-7 fold lower affinity for double-stranded B-DNA. The sequence specificity of the observed interactions was not examined. The observations that antiserum versus mouse ζ-crystallin reacts specifically with the 36-kDa protein contained in the purified pH-RE binding protein and blocks formation of the specific complex formed with the pH-RE indicates that the ζ-crystallin/NADPH:quinone reductase also has a high affinity binding site for the AU-rich pH-RE.

Previous to this study, other proteins of the dehydrogenase family (glyceraldehyde-3-phosphate dehydrogenase, lactate dehydrogenase, yeast mitochondrial NAD^+-dependent isocitrate dehydrogenase, and glutamate dehydrogenase) and other $NAD(P)^+$/NAD(P)H-binding enzymes (catalase and dihydrofolate reductase) were demonstrated to have sequence-specific RNA binding activity. It was proposed that their active sites, which bind either form of pyridine dinucleotides, exhibit a common pattern of two βαβαβ-units known as a dinucleotide-binding fold or a Rossmann fold. In glyceraldehyde-3-phosphate dehydrogenase, the RNA-binding site has been located within the NAD^+-binding domain, not the catalytic domain. This specific binding affinity is diminished by addition of NAD^+, NADH or ATP. Similarly, the DNA-binding ability

of ζ-crystallin is effectively competed by NADPH (Gagna, 1998). Thus, the NADPH binding site of ζ-crystallin may constitute a portion of the pHRE binding site.

6.3 Expression of recombinant ζ-crystallin.

ζ-crystallin cDNA was inserted into two different vectors. In pET-3a, expression was not as successful as in pET-15b. This could result from the use of the T7lac promoter in pET-15b, as compared to the T7 promoter in pET-3a, to drive ζ-crystallin expression. As a result, in pET-15b-zeta, recombinant expression was significantly higher after IPTG induction. However, even though over-expression was confirmed in a western experiment, a crude extract from *E. coli* containing the highly expressed protein failed to demonstrate increased binding activity to the R-2I RNA. To rule out the possibility that the extra N-terminal sequence distorted the protein structure, this extract was purified using its His-tag and then cleaved using the thrombin cleavage site (data not shown). The cleavage was confirmed on a silver-stained SDS-PAGE. However, the purified and cleaved protein again failed to bind the R-2I RNA. Thus, a eukaryotic post-translational modification may be necessary to impart pHRE-binding activity.

In an RNA-EMSA, an extract from *E. coli* was able to form a high affinity complex with the R-2I RNA. Formation of such complex was observed with cells transformed with only pET-3a or pET-15b. Thus, the binding protein must be an endogenous protein from *E. coli* whose identity is not known. The protein could be the bacterial counterpart of NADPH:quinone reductase or another protein with a similar Rossmann fold.

Expression in LLC-PK_1-F^- cells yielded supportive but ambiguous data. These cells contain an RNase activity that could not be effectively inhibited by RNAsin. WKPT cells are a rat cell line that was isolated from proximal tubules. When transferred to acidic medium, its 4.7-kb GA mRNA is increased by 3-fold. Furthermore, its endogenous RNase activity can be inhibited by RNAsin addition. In future experiments, expression will be done in WKPT cells to examine the interaction between ζ-crystallin and R-2I.

6.4 Future experiments

So far our results fit into the following hypothesis (Fig. 6.1): The AU-rich element in the GA mRNA 3'-UTR serves as a site for RNase digestion. At the same time, it binds to ζ-crystallin with a high affinity. In normal acid-base balance, the weak binding of ζ-crystallin allows for the rapid degradation of the GA mRNA. During acidosis, the increased affinity from ζ-crystallin blocks the endonucleolytic cleavage, which leads to the stabilization of the mRNA and upregulation of GA expression. Another possibility exists that during normal condition, the AU-rich element recruits another protein that interacts with the poly(A) tail and accelerates deadenylation. The onset of acidosis causes ζ-crystallin to displace this protein and stabilizes that mRNA. Distinction of the two possibilities requires characterization of the GA mRNA degradation pathway.

An appropriate expression vector for ζ-crystallin will be constructed and used to transfect WKPT cells. After over-expression is confirmed by a western analysis, cytosolic extracts will be prepared and used in an RNA-EMSA to examine the ability to bind the R-2I RNA. This result will be compared with that obtained with non-transfected cells. This should further confirm that ζ-crystallin is the pHRE-BP.

Fig. 6.1. Model for regulation of GA mRNA during acidosis.

Under normal conditions (pH 7.4), there is less ζ-crystallin that forms a complex with GA mRNA. Therefore an RNase may access this site and initiate degradation more easily. Acidosis causes an increased binding and protects the GA mRNA.

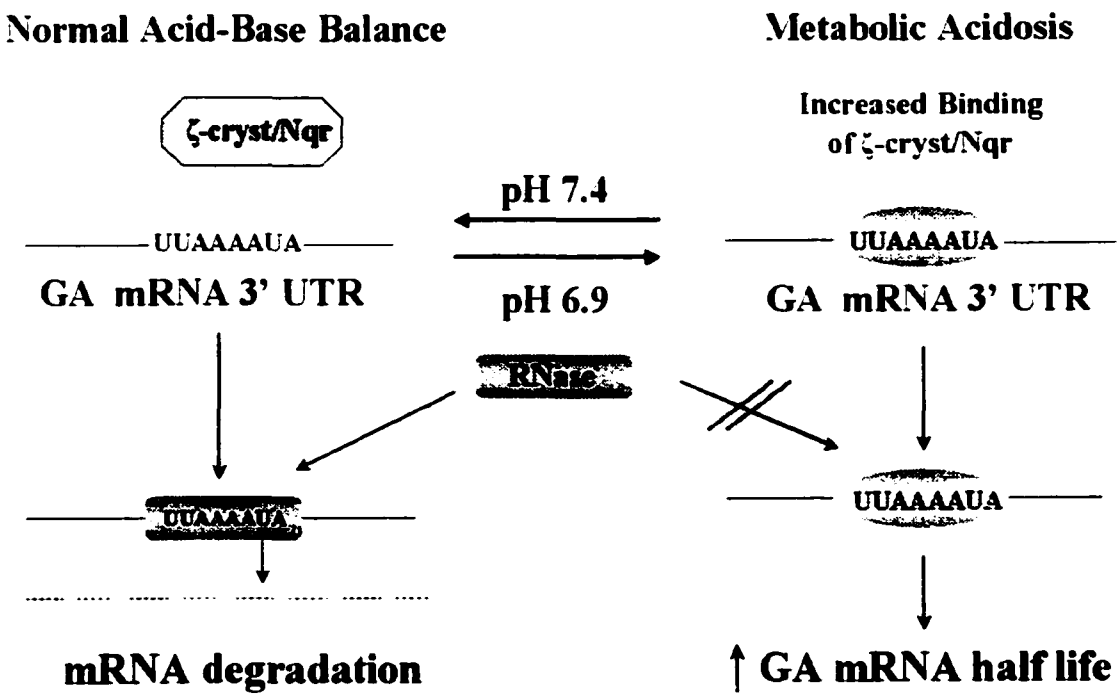

Fig. 6.1

The turnover rate of the 4.7-kb GA mRNA will be studied in both the transfected cells and control cells using normal medium. This will be accomplished by using DRB to inhibit RNA production, and monitoring the degradation of the GA mRNA by northern blotting. If our model truly reflects what occurs during acidosis, we should see that the 4.7-kb GA mRNA in transfected cells degrades at a slower rate. Similar result should be observed by transferring the non-transfected cells to acidic medium. This should further enhance the stability of the GA mRNA and lead to a greater increase in GA activity.

The amino acid sequence of ζ-crystallin will be compared with the known Rossmann fold sequence. If an alignment is found, deletion constructs will be made so that the NADPH binding site is intact. This shortened sequence will be integrated into an expression vector to transfect WKPT cells. Extract will be made to examine its affinity to pHRE.

6.5 Signal transduction pathway – the big picture.

In LLC-PK_1-F^+ cell, p38 adaptation parallels PEPCK induction during acidosis. Anisomycin, a strong p38 activator, increases the level of PEPCK and GA mRNAs without the addition of acidic medium. SB203580, a p38-specific inhibitor, is able to block the effect of anisomycin or acidic medium on induction of the PEPCK mRNA. Surprisingly, addition of SB203580 does not affect GA adaptation. Thus PEPCK and GA are coordinately regulated through a signaling pathway that may have the same upstream signal that diverges to separately regulate transcriptional and post-transcriptional processes. At the p38 level, four isoforms can be activated by similar phosphorylation by MKK3 and MKK6. However, in LLC-PK_1-F^+ cell, only the α isoform is strongly

expressed. This isoform, which is likely to take part in PEPCK regulation, is inhibited by SB203580. Thus, none of the 4 known isoforms of p38 is likely to be involved in regulation of GA mRNA stability.

Other MAPKs were tested as well. In A431 and Swiss 3T3 cells, a low extracellular pH (maximal response at pH 4 to 5) induces activation of ERK2, JNK, and p38. In LLC-PK_1-F^+ cell, ERK1/2 inhibitors (PD098059 and U0126) did not affect basal or acid-induced levels of PEPCK mRNA. An acidic environment caused a decrease in JNK phosphorylation, and the JNK inhibitor curcumin also had no effect on levels of PEPCK mRNA. The role of ERK5 in GA regulation, or other MAPKs in acidosis has not been tested.

It is possible that the upstream activators of p38, MKK3 or MKK6, may directly phosphorylate ζ-crystallin (Fig. 6.2). MAPK pathways are generally organized in tiered cascades where one kinase phosphorylates its downstream kinases. High specificity is observed, especially at the level of MAPKKs activation of MAPKs. However, crosstalk often occurs to give rise to more complex pathways. For example, TAK, ASK1 and MLK3 (all MAPKKKs) can activate both MKK4, 7 (which leads to JNK1-3 activation) and MKK3, 6 (which leads to activation of p38 isoforms). Both branches lead to activation of ATF-2. Without further evidence, it is hard to propose a specific signaling pathway that regulates GA mRNA stability. Progress in understanding the regulation of PEPCK may shed light on this study.

Aside from phosphorylation of ζ-crystallin itself, its affinity may be affected by other changes, such as other covalent modifications, conformational changes, or binding to other molecules. The only preliminary experiment completed in this regard showed

that potato acid phosphatase (PAP) treatment did not affect apparent binding to R2-1 of ζ-crystallin from either normal or acidotic rat renal cytosolic extracts.

Transcription of ζ-crystallin is another possible site of regulation during acidosis. A study of this kind will require cloning of ζ-crystallin promoter region from rat kidney and characterizing its transcription rate during normal and acidotic conditions.

Fig. 6.2. Possible signal pathway that is activated during acidosis.

ERK1/2 and JNK are not likely to be involved in pH-response. During acidosis the MKK3/6 –> p38 –> ATF2 pathway is activated to enhance PEPCK transcription. ζ-crystallin may be phosphorylated by a kinase that is upstream of p38.

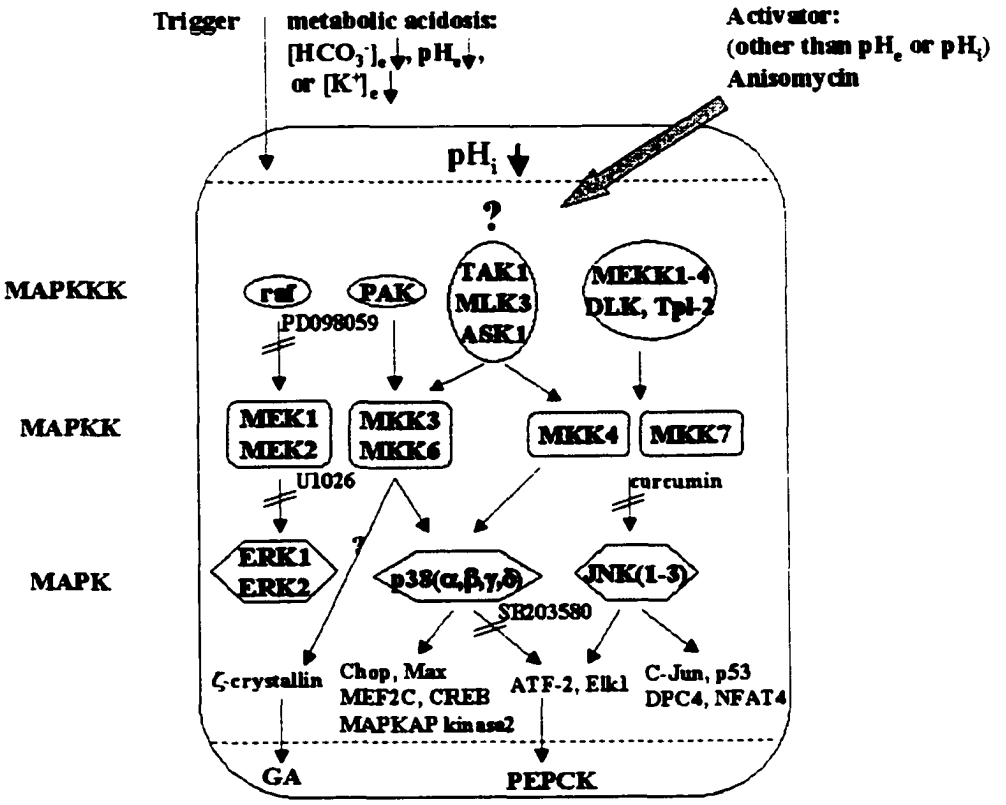

Fig. 6.2

7. References

7. REFERENCES

Bachurski., C. J., Theodorakis, N. G., Coulson, R. M., Cleveland, D. W., *Mol. Cell. Biol.* 14: 4076-4086, 1994.

Bradford, M. M., *Anal. Biochem.* 72: 248-252.

Bradford, H. F., Ward, K. H., and Thomas, A. J., *J. Neurochem.* 30:1453-59, 1978.

Brewer, G., *Mol. Cell. Biol.* 11: 2460-2466, 1991.

Brosnan, J. T., P. Vinay, A. Gougoux, and M. L. Halperin. In: *pH Homeostasis-Mechanism and Control,* edited by D. Häussinger. New York: Academic Press, p. 281-304, 1988.

Burch, H. B., R. G. Narins, C. Chu, S. Fagiolo, S. Choi, W. McCarthy, and O. H. Lowry. *Am. J. Physiol.* 235: F246-F253, 1978.

Chang, L. and Karin, M. *Nature.* 410: 37-40. 2001.

Chen, C. Y., and Shyu, A. B., *Trends Biochem. Sci.,* 20: 465-470, 1995.

Chen, C. Y., Gherzi, R., Anderson, J. S., Gaietta, G., Jurchott., K.,Royer, H. D., Mann, M., Karin, M., *Genes Dev.* 14: 1236-1248, 2000.

Cheong, J. H., J. E. Coligan, and J. D. Shuman. *J. Biol. Chem.* 273: 22714-22718, 1998.

Chittum, H. S., Lane, W. S., Carlson, B. A., Rollar, P. P., Lung, P. D., Lee, B. J., and Hatfield, D. L. *Biochemistry* **37,** 10866-10870, 1998

Colgan, D. F., and Manley, J. L. *Genes & Development.* 11:2755-2766, 1997.

Colquhoun, A., and E. A. Newsholme. *Biochem. Mol. Biol. Int.* 41: 583-596, 1997.

Curthoys, N. P., and O. H. Lowry. *J. Biol. Chem.* 248: 162-168, 1973.

Curthoys, N. P., and M. Watford. Regulation of glutaminase activity and glutamine metabolism. *Annu. Rev. Nutr.* 15: 133-159, 1995.

Curthoys, N. P., and Gstraunthaler, G., *Am. J. Physiol. Renal Physiol.* 281: F381-F390, 2001.

Dember, L. M., Kim, N. D., Liu, K. and Anderson, P., *J. Biol. Chem.*, 271: 2783-2788, 1996.

Dixon, D. A., Kaplan, C. D., McIntyre, T. M., Zimmerman, G. A., Prescott, S. M., *J. Biol. Chem.* 275:11750-11757. 2000.

Drewnowska K., W. T. Labruyere, M. J. B. van den Hoff, W. H. Lamers, and A. C. Schoolwerth. *Contrib. Nephrol.* 121: 25-30, 1997.

Feifel, E., S. Euler, P. Obexer, A. Tang, Y. Wei, H. Schramek, N. P. Curthoys, and G. Gstraunthaler. submitted to *Am. J. Physiol. Renal Physiol.*

Fournier, B., Truong-Bolduc, Q. C., Zhang, X., and Hooper, D. C., *J. Bacteriol.* 183: 2367-2371, 2001.

Gagna, C. E., J. H. Chen, H.-R. Kuo, and W. C. Lambert. *Cell Biol. Int.* 22: 217-225, 1998.

Garland, D., P. V. Rao, A. Del Corso, U. Mura, and J. S. Zigler, Jr. *Arch. Biochem. Biophys.* 285: 134-136, 1991.

Gebhardt, R., Mecke, D. *EMBO J.* 2: 567-570, 1993.

Gonzalez, P., C. Hernandez-Calzadilla, P. V. Rao, I. R. Rodriguez, J. S. Zigler, Jr., and T. Borras. *Mol. Biol. Evol.* 11: 305-315, 1994.

Gonzalez, P., Rao, P. V., Nunez, S. B., and Zigler, J. S., *Mol. Biol. Evol.* 12(5): 773-781, 1995.

Good, D. W., and M. B. Burg. *J. Clin. Invest.* 73: 602-610, 1984.

Graves, L. M., *Nature*, 403: 328-332, 2000.

Grosset, C., Chen, C.A., Xu, N., Sonenberg, N., Jacquemin-Sablon, H., and Shyu, A-B., *Cell.* 103: 29-40, 2000.

Grunberg-Manago, M. *Annu. Rev. Genet.* 33: 193-227, 1999.

Guhaniyogi, J. and Brewer, G. *Gene.* 265: 11-23, 2001.

Gueydan, C., Droogmans, L., Chalon, P., Huez, G., Caput, D., and Kruys, V., *J. Biol. Chem.*, 274: 2322-2326, 1999.

Han, J, Jiang, Y., Li, Z., Kravchenko, V. V., and Ulevitch, R. J., *Nature*, 386: 296-299, 1997.

Hansen, W. R., N. Barsic-Tress, L. Taylor, and N. P. Curthoys. *Am. J. Physiol. Renal Fluid Electrolyte Physiol.* 271: F126-F131, 1996.

Haussinger, D. *Adv. Enzymol. Relat. Areas Mol. Biol.* 72: 43-86, 1998.

Hentze M. W. *Trends Biochem. Sci.* 19: 101-103, 1994.

Holcomb, T., W. Liu, R. Snyder, R. Shapiro, and N. P. Curthoys. *Am. J. Physiol. Renal Fluid Electrolyte Physiol.* 271: F340-F346, 1996.

Horie, S., O. Moe, A. Tejedor, and R. J. Alpern. *Proc. Natl. Acad. Sci. USA* 87: 4742-4745, 1990.

Hughey, R. P., B. B. Rankin, and N. P. Curthoys. *Am. J. Physiol.* 238: F199-F204, 1980.

Hwang, J-J., and N. P. Curthoys. *J. Biol. Chem.* 266: 9392-9396, 1991.

Hwang, J-J., S. Perera, R. A. Shapiro, and N. P. Curthoys. *Biochemistry* 30: 7522-7526, 1991.

Jacobson, A. and Peltz, S.W. *Annu. Rev. Biochem.* 65: 693-739. 1996.

Jaiswal, A.K. *Pharmacogenetics.* 4: 1-10. 1994.

Kallunki, T.,Deng, T., Hibi, M., and Karin, M., *Cell.* 87: 929-939. 1996.

Kawakami, A., Tian, Q., Duan, X., Streuli, M., Schlossman, S. F., and Anderson, P., *Proc. Natl. Acad. Sci. USA.* 89: 8681-8685, 1992.

Kvamme, E. *Glutamine metabolism in mammalian tissue.* Springer-Verlag, Berlin pp. 33-48, 1984.

Laterza, O. F., and N. P. Curthoys. *Am. J. Physiol. Renal Physiol.* 278: F970-F977. 2000.

Laterza, O. F., and N. P. Curthoys. *J. Am. Soc. Nephrol.* 11: 1583-1588, 2000.

Laterza, O. F., Ph. D. thesis, 1998.

Laterza, O. F., W. R. Hansen, L. Taylor, and N. P. Curthoys. *J. Biol. Chem.* 272: 22481-22488, 1997.

Lavery, D. J. Schibler, U., *Genes Dev.* 7:1871-1884. 1993.

Lee, D. C., P. Gonzalez, and G. Wistow. *J. Mol. Biol.* 236: 669-678, 1994.

Lowry, M., and B. D. Ross. *Biochem. J.* 190: 771-80, 1980.

Ma, W. J.,Cheng, S., Campbell, Cl, Wright, A., and Furneaux, H., *J. Biol. Chem.*, 271: 8144-8151, 1997.

McCauley, R., S. E. Kong, K. Heel, and J. C. Hall. *Int. J. Biochem. Cell Biol.* 31: 405-413, 1999.

Nagy, E., and Rigby, W. F., *J. Biol. Chem.*, 270: 2755-2763, 1995.

Neu, J., Shenoy,V., and Chakrabarti, R. *FASEB J.* 10: 829-837, 1996.

Newsholme, E. A., and P. C. Calder. *Nutrition* 13: 728-730, 1997.

Noshiro, M., Nishimoto, M., Okuda, D., *J. Biol. Chem.* 265:10036-10041. 1990.

Ono, K. Han, J. *Cellular signaling* 12:1-13. 2000.

Paulding, W. R., Czyzyk-krzeska, M. F., *Adv. Exp. Med. Am. J. Physiol. Renal Fluid Electrolyte Physiol.* 269: F363-F373, 1995.

Preisig, P. A., and R. J. Alpern. *J. Clin. Invest.* 82: 1445-1453, 1988.

Raghow, R., Gossage, D., Kang, A. H., *J. Biol. Chem.* 261:4677-4684. 1986.

Raghow, R., Postlethwaite, A. E. Keski-Oja, J., Moses, H. L., Kang, A. H., *J. Clin. Invest.* 1285-1288. 1987

Rao, P. V., P. Gonzales, B. Persson, H. Jörnvall, D. Garland, and J. S. Zigler, Jr. *Biochemistry* 36: 5353-5362, 1997.

Ross, A. F., Oleynikov, Y., Kislauskis, E. H., Taneja, K. L. and Singer, R. H. *Mol. Cell. Biol.* 17: 2158-2165, 1997.

Ross, J., *TIG.* 12:171-175, 1996.

Rouault, T. A., Hentze, M. W., Haile, D. J., Harford, J. B., and Klausner, R. D., *Proc. Natl. Acac. Sci. USA.* 86: 5768-5772, 1989.

Rouault, T., and Klausner, R., *Curr. Top. Cell. Regul.* 35: 1-19, 1997.

Sajo, I. M., M. B. Goldstein, H. Sonnenberg, B. J. Stinebaugh, D. R. Wilson, and M. L. Halperin. *Kidney Int.* 20: 353-358, 1981.

Sambrook, J., Fritsch, E. F., and Maniatis, T., *Molecular Cloning: A laboratory Manual,* 2nd Ed., pp.6.1-6.48, Cold Spring Harbor Laboratory, Cold Spring Harbor, NY.

Sastrasinh, M., and S. Sastrasinh. *Am. J. Physiol.* 259: F863-866, 1990.

Schiavi, S. C., Belasco, J. G., and Greenberg, M. E., *Biochim. Biophys. Acta.* 1114: 95-106. 1992

Schrock, H., C. J. Chu, and L. Goldstein. *Biochem. J.* 188: 557-560, 1980.

Shapiro R. A., Haser, W. G., and Curthoys, N. P., *Biochem. J.*, 1987.

Shapiro, R. A., Farrell, L., Srinivasan, M., and Curthoys, N. P., *J. Biol. Chem.* 266:18792-96, 1991.

Short, S., Tian, D., Short, M. L., Jungmann, R. A., *J. Biol. Chem.* 276:12963-12969. 2000.

Silbernagl, S. *Int. J. Biochem.* 12: 9-16, 1980.

Squires, E. J., D. E. Hall, and J. T. Brosnan. *Biochem. J.* 160: 125-128, 1976.

Srinivasan, M., Kalousek, F., Curthoys, N. P., *J. Biol. Chem.* 210:277-280, 1995.

Tang, A., and N. P. Curthoys. *J. Biol. Chem.* 276: 2001, in press.

Tannen, R. L. In: *Handbook of Physiology. Renal Physiology*, edited by J. Orloff and R.W. Berliner. Oxford, UK: Oxford Univ. Press, 1993, Vol. I, Sect. 8, Chapt. 23, p. 1017-1059.

Taupin, J., Tian, Q., Kedersha, N., Robertson, M., and Anderson, P., *Proc. Natl. Acad. Sci. USA.* 92: 1629-1633, 1995.

Tong, J., R. A. Shapiro, and N. P. Curthoys, *Biochemistry* 26: 2773-2777, 1987.

Watford, M., Smith, E. M. *Biochem. J.* 267:265-267, 1990.

Watford, M., *Biochim. Biophys. Acta* 1200:73-78, 1994.

Weiler, C. T., Nystrom, B., and Hamberger, A., *Brain Res.* 160:539-43, 1979.

Whitfield, M. L., Zheng, L. X., Baldwin, A., Ohta, T., Hurt, M. M., and Marzluff, W. F., *Mol. Cell. Biol.* 20: 4188-4198, 2000.

Wright, P. A., and M. A. Knepper. *Am. J. Physiol.* 259: F961-F970, 1990.

Xu, N., Chen, C.A., and Shyu, A-B., *Mol. Cell. Biol.* 17(8): 4611-4621, 1997.

Xue, L. and Lucocq, J.M. *Biochem. Biophys. Res. Commun.* 241(2): 236-242. 1997.

Yeilding, N. M., Lee, W. M., Mol. Cell. Biol. 17:2698-2707. 1997.